CHAPTER THREE

Evolving in the Community

On your hikes through nature, if you stop and ponder the features of any species you encounter, you will quickly realize that many of those features are critical for how it interacts with its environment. Many traits permit the organism to cope with the physical features of the environment it encounters. Waxy cuticles of leaves and insects reduce evaporative water loss. Lamellar gills permit aquatic insects to extract oxygen from the water.

Other traits shape how the individual will interact with individuals of its own and other species. The long proboscis of a butterfly and the extended bill of a hummingbird allow them to extract nectar from flowers with long corollas. Snails have shells that protect them from many predators, but the crushing pharyngeal jaws of a pumpkinseed sunfish permit it to feast on those snails. Tadpoles of many frog species have noxious chemicals that make them distasteful to many predators, but these toxins do not deter the few predators that lack taste receptors for the chemicals. Some prey can move rapidly to evade attacking predators, but others remain motionless and cryptic in order to not be seen.

The abilities of species to engage in interactions with the environment and other species are defined by the phenotypes they possess. Presumably, many of these taxa acquired their collection of traits through evolution in response to the pressures of natural selection generated by interactions with their physical environment and other species in this community. In other words, these species evolved traits to exploit the ecological opportunities available to them.

These ecologically important traits are what determine the parameters of the models we considered in chapter 2. The butterfly with a longer proboscis will be able to extract more nectar from flowers with longer corollas, and will therefore have a higher attack coefficient for harvesting this resource. Likewise, a damselfly larva that moves very little to remain cryptic will have a lower attack coefficient from foraging fish than a damselfly larva that moves more and thus is seen more easily by the fish. However, the damselfly larva that moves less will also have a lower attack coefficient on its own prey because it encounters them at a lower rate than the one that moves more.

Thus, a reciprocity exists between the ecological structure in which a species is embedded, and the evolutionary dynamics of it and all the other species

with which it interacts. The phenotype of a species defines how successful, in demographic terms, a species will be in the various interactions in which it must engage. These performance abilities in turn are what determine all the parameters of the models we considered in chapter 2 that delineate whether the species can coexist in a particular community. In addition, variation in demographic success among individuals within that species also defines the nature of natural selection acting on that species, and so defines the evolutionary trajectory of that species. Because all species are evolving in response to one another, we must think of this as a coevolutionary dynamic (Thompson 1994, 2005). As one species evolves, its demographic impact on other species in the community change, and in turn alters their evolutionary trajectories. While coevolutionary dynamics may not be ongoing—the system may have reached stable evolutionary equilibria for the phenotypes of all species—the interactions among species are what determine where these evolutionary equilibria are located. Thus, the reciprocal coevolutionary responses among species and the ultimate evolutionary outcomes are defined by the ecological structure of the community. The changing nature and abilities of the actors in the ecological theater animate the evolutionary play.

THE ECOLOGICAL BASIS OF NATURAL SELECTION

Natural selection, the struggle for existence of different types within a species, as first outlined by Charles Darwin and Alfred Russel Wallace (Darwin and Wallace 1858), is essentially the demography of phenotypes and genotypes within and among populations. The process of natural selection has two components (Endler 1986). The first is phenotypic selection, in which the phenotypic distribution in the parental generation is changed because of differential survival or reproduction based on the phenotypic properties of individuals (or a collection of individuals if higher-level selection is being considered). The second is the genetic response to this phenotypic selection.

In most theoretical considerations of natural selection, the focus is placed squarely on the mechanisms involved in the genetic response to selection, and many simplifying assumptions are made about phenotypic selection and its underlying cause. This is typically done so that complex genetic interactions can be explored. In general, how the fitnesses of various members of the population are determined is ignored completely by merely assigning constant fitness values to various genotypes or phenotypes in the population.

However, the fitness of an individual is determined by the ecological conditions in which the individual is embedded and will therefore change as those ecological conditions change. Consequently, the relationship between fitness and phenotype has dynamics that are governed by the ecology of the system. “The ecology of the

system" is not some external set of conditions imposed on these species but rather is defined by how the phenotypes of the interacting species determine the parameters of their interaction. For example, the ability of a dragonfly to catch a damselfly depends on the phenotypic traits of these two individuals, and the population level parameters determining the attack coefficient of the dragonfly predator on its damselfly prey depend on the distribution of phenotypes in the populations of both these interacting species.

Moreover, as the phenotypic distribution of one species evolves, the fitness consequences of interacting with that species will also change. If over one generation the damselfly population evolves to swim faster because of selection pressures imposed by dragonfly predation, in the next generation, the attack coefficient between this predator and prey will be smaller. As a result, the fitnesses of dragonflies with a particular value of a phenotypic trait for feeding on these damselflies will decrease. If the dragonfly population then evolves to be faster at pursuing the damselfly in the next generation, the attack coefficient between them will increase again.

These considerations lead inexorably to the conclusion that the ecological dynamics of the evolutionary process are fundamental to understanding the outcomes of that process. Therefore, in the analyses presented here, I turn the tables by allowing the ecological mechanisms defining natural selection to have full reign, and having the simplifying assumptions made about the genetics of the system. This is in essence the basis of quantitative genetic analyses (Falconer and Mackay 1996, Lynch and Walsh 1998). Thus, I focus on how the ecological dynamics of natural selection influence what will coevolve in a community of interacting species.

For natural selection to occur, three criteria must be met. First, some trait or traits expressed by individuals in a population must influence their survival or reproduction (i.e., their fitness). Second, individuals in the population must vary in these traits that cause fitness differences among them. Third, these trait differences must have a heritable genetic basis. The first and second criteria identify the conditions needed for phenotypic selection to occur, and the third criterion establishes that the population will genetically change in response to phenotypic selection.

The general term "fitness" is used in many, many different ways, and the debate about what is the "correct" fitness measure to consider often obscures the issues more than clarifies. When the ecological dynamics of natural selection are explicitly explored, the *absolute fitness* of an individual is the foundational metric underlying the dynamics of selection. This is because absolute fitness is the central mediating parameter between the evolutionary dynamics caused by natural selection and the demography of a population. Absolute fitness is defined as the number of offspring contributed to the next generation by an individual.

An individual's absolute fitness is the demographic consequence of the interaction of the individual's phenotype with its ecological environment. The

environment includes the abiotic conditions experienced by the individual as well as all the interactions with conspecifics and other species. Fundamentally, *absolute fitness is an ecological property*. If all individuals in a population have identical phenotypes, the fitness of each individual would precisely describe the dynamics of the population. In other words, the overall dynamics of the population would be simply the fitness of each individual times the number of individuals in the population, or

$$\frac{dN_i}{dt} = N_i \ln(W_i) = N_i \frac{dN_i}{N_i\, dt}, \tag{3.1}$$

where N_i is the number of individuals in the population of species i, and $\ln(W_i)$ is the logarithm of the absolute fitness of each individual; this product is equivalent to the per capita population growth rate $dN_i/N_i\, dt$ (see chapter 2). (Because the modeling framework utilized here is a continuous time frame using differential equations, absolute fitness is measured on a log scale, where individuals are just replacing themselves at $W_i = 1$ so that $\ln(W_i) = 0$.) One interpretation of these equations implies that the population dynamic models used in chapter 2 assume that each species is composed exclusively (or at least predominantly) of only one phenotype. (See table 3.1 for a complete list of state variables and parameters used in models in this chapter.)

However, a little algebra shows that even if the population is composed of individuals that vary in their demographic rates because their phenotypes vary, the overall population growth rate has a rational interpretation. First, define the number of species i individuals having phenotypes in the infinitesimal range $z_i + dz_i$ to be $n_i(z_i)$, total population size to be $N_i = \int n_i(z_i)\, dz_i$, and the absolute fitnesses of individuals in this infinitesimal phenotypic range are $W_i(z_i)$ (as in Lande 2007). The total population growth rate is then given by

$$\frac{dN_i}{dt} = \int n_i(z_i) \ln(W_i(z_i))\, dz_i. \tag{3.2}$$

Defining the frequency of individuals in each narrow phenotypic range to be $p_i(z_i) = n_i(z_i)/N_i$, we can arrange this equation to be

$$\frac{dN_i}{dt} = \frac{N_i}{N_i} \int n_i(z_i) \ln(W_i(z_i))\, dz_i = N_i \int p_i(z_i) \ln(W_i(z_i))\, dz_i. \tag{3.3}$$

The integral in this equation is the average fitness in the population: $\ln(\bar{W}_i) = \int p_i(z_i) \ln(W_i(z_i))\, dz_i$. For completeness, this means that

$$\frac{dN_i}{dt} = N_i \int p_i(z_i) \ln(W_i(z_i))\, dz_i = N_i \ln(\bar{W}_i) = N_i \frac{dN_i}{N_i\, dt}. \tag{3.4}$$

TABLE 3.1. Additional state variables and parameters in the evolutionary models of species interactions presented. Variables and parameters that are common to multiple species types are shown for only the resource species. All other variables and parameters are as listed in table 2.1.

State Variable	*Description*
z_R, z_N, z_P	Traits of the resource, consumer, and predator species, respectively
$\bar{z}_R, \bar{z}_N, \bar{z}_P$	Mean trait values of species
$R(z_R), N(z_N), P(z_P)$	Population abundances of species with the associated trait values
$W_R(z_R), W_N(z_N), W_P(z_P)$	Absolute fitnesses of species with the associated trait values
$\Delta = z_N - z_R$	Difference between the consumer and resource trait values
$\Omega = z_P - z_N$	Difference between the predator and consumer trait values
$\Sigma = z_P - z_R$	Difference between the predator and resource trait values
Parameter	*Description*
$V_{z_R}, V_{z_N}, V_{z_P}$	Additive genetic variation for traits in the three species
c_0	Maximum value for the resource species' intrinsic birth rate
$\tilde{z}_R^c$	Optimal trait value for the intrinsic birth rate of the resource species
γ	Scaling parameter for the underlying selection strength on the resource's intrinsic birth rate
d	Density-dependent rate of decrease in the resource's birth rate
f_0, x_0	Minimum value for the intrinsic death rates of the consumer and predator, respectively
θ, δ	Scaling parameters for the underlying selection strengths on the intrinsic death rate of the consumer and predator, respectively
g, y	Density-dependent rates of increase in the intraspecific death rates of the consumer and predator, respectively
$\tilde{z}_N^f, \tilde{z}_P^x$	Optimal trait value for the intrinsic death rates of the consumer and predator, respectively
a_0	Maximum value of the attack coefficient of the consumer feeding on the resource
$\varepsilon_i, \alpha, \beta$	Scaling parameters for the rate of change in the attack coefficient of the consumer feeding on the resource for the unidirectional-independent, unidirectional-dependent, and bidirectional-dependent trait interactions, respectively
m_0	Maximum value of the attack coefficient of the predator feeding on the consumer

(*continued*)

TABLE 3.1. (*continued*)

State Variable	*Description*
η_i, ρ, ϕ	Scaling parameters for the rate of change in the attack coefficient of the predator feeding on the consumer for the unidirectional-independent, unidirectional-dependent, and bidirectional-dependent trait interactions, respectively
v_0	Maximum value of the attack coefficient of the predator feeding on the resource
κ_i, τ, ψ	Scaling parameters for the rate of change in the attack coefficient of the predator feeding on the resource for the unidirectional-independent, unidirectional-dependent, and bidirectional-dependent trait interactions, respectively

In words, the per capita population growth rate of the population is equivalent to the average fitness of individuals in the population: $dN_i/N_i\,dt = \ln(\bar{W}_i)$ (Lande 2007).

In chapter 2, we saw how the population growth rate of a species was influenced by interactions with other species in the local community, but none of the species could evolve in response to one another. Equation (3.4) implies that these influences are mediated through their effects on the absolute fitnesses of individuals that constitute the local population of that species. Moreover, because the fitnesses of those individuals are determined by how their phenotypes demographically translate these interactions into absolute fitness, overall population growth rate depends on the phenotypic composition of the population, $p_i(z_i)$. *The per capita population growth rate is the average absolute fitness of individuals in the population.* Given these relationships, it should be apparent that we can use the ecological machinery describing the population dynamics of interacting species from chapter 2 as a descriptor of how species interactions influence the absolute fitness of each species within a local community, and thus the ecological dynamics of natural selection for each. This provides the fundamental link between ecological and evolutionary dynamics, since the basis of both are defined by how ecological interactions shape absolute fitness.

If we expand our expression for absolute fitness to represent all the influential species interactions, the complexity of fitness dynamics becomes apparent. For example, in this framework we can represent the per capita effects of various species interactions on the absolute fitnesses of individuals with phenotype z_i within species i as

$$\ln(W_i(z_i)) = \sum_j N_j \int p_j(z_j) f_{ij}(z_i, z_j)\, dz_j. \tag{3.5}$$

Here $f_{ij}(z_i, z_j)$ are functions describing the per capita effect of various phenotypic classes within species j on the absolute fitness of an individual of species i, and $p_j(z_j)$ are the frequencies of individuals in the various phenotypic classes. These per capita effects may depend on the phenotypes of both species. Note that equation (3.5) includes both the effects of species i on itself (i.e., intraspecific effect when $j = i$) and the effects of other species on species i (i.e., interspecific effects when $j \neq i$). The effect of species j on the fitness of individuals of species i represents a *fitness component* that contributes to the *overall absolute fitness* of species i. Fitness components are typically considered to be associated with life stages, but this interpretation separates fitness into components due to the action of different selective agents on various demographic rates (e.g., survival of resource i due to predation by consumer j).

Equation (3.5) also describes the *fitness surface* defined by the ecological environment in which the population of species i is embedded at any given instant. This equation immediately identifies that the shape of the fitness surface of each species will vary with both the phenotypes and abundances of all species in the community, meaning that analyses of natural selection that assume fixed fitnesses associated with various types (genotypes or phenotypes) in the population ignore the rich ecological dynamics that govern the process. This equation also highlights the fact that the shape of the overall fitness surface depends on the contributions of the various underlying fitness components (Arnold and Wade 1984b, Travis 1989, Wade and Kalisz 1990, McPeek 1996a). The relative importance of each species interaction to determining the shape of the overall fitness surface will depend on both the magnitudes of the per capita effects and the abundances of the various species.

Many different modeling approaches can be taken to explore the dynamics of trait change in interacting populations. In principle, one could take a population genetic approach, but this becomes exceedingly opaque and cumbersome when fitnesses are density and frequency dependent (Nagylaki 1992), which is why I will make simplifying assumptions about the genetics of the system. An alternative that has many appealing features is the adaptive dynamics approach (Dieckmann and Law 1996, Doebeli 2011). With adaptive dynamics, a population is assumed to contain one genetic type of individual. At each step in time, individuals with slightly different phenotypes (and genotypes) are assumed to invade the population at low frequency (e.g., as mutations from the dominant type), and the population changes if these invading individuals have fitnesses higher than the dominant type. Adaptive dynamics approaches have been applied to questions of behavioral choice among individuals in a population (e.g., Eshel 1981a, 1981b), adaptive evolution in interacting species (e.g., Dieckmann and Law 1996), and sympatric speciation (e.g., Doebeli and Dieckmann 2000).

I will utilize the approach developed by Lande (1982) and elaborated by Iwasa et al. (1991) and Abrams et al. (1993) (see also Lande 2007, Barfield et al. 2011), which models the evolution of quantitative traits in the same framework used by empirical biologists to study natural selection in the wild (Lande 1979; Lande and Arnold 1983; Arnold and Wade 1984b, 1984a). Thus, results of these analyses should provide testable predictions about species interactions and natural selection that can be directly tested in the field. Under the standard assumptions of the genetic basis of quantitative traits (i.e., many loci, each of small effect) and of traits and breeding values being normally distributed, the dynamics of natural selection are closely approximated by the dynamics of the average phenotypic *trait value* in the population ($\bar{z}_i$); since population dynamics are defined by the average fitness (equation (3.5)), this assumption further associates the average fitness of the population with the average phenotype in the population (Lande 1982, 2007). This framework can be further simplified by assuming that the effects of interactions with species *j* are primarily defined by the effects of individuals with the average phenotype ($\bar{z}_j$). Thus, equation (3.5) becomes

$$\ln(W_i(z_i)) = \sum_j N_j f_{ij}(z_i, \bar{z}_j). \tag{3.6}$$

In this framework, the evolutionary dynamics of the mean trait in the population is given by

$$\frac{d\bar{z}_i}{dt} = V_{z_i} \frac{\partial \ln(W_i(z_i))}{\partial z_i}\bigg|_{z_i=\bar{z}_i} = V_{z_i}\left(\sum_j N_j \frac{\partial f_{ij}(z_i, \bar{z}_j)}{\partial z_i}\bigg|_{z_i=\bar{z}_i}\right), \tag{3.7}$$

where the partial derivatives with respect to z_i are evaluated at the mean trait value $\bar{z}_i$, and V_{z_i} is the additive genetic variance among individuals in the population for the trait (Lande 1982, Iwasa et al. 1991, Abrams et al. 1993). The appendix in Iwasa et al. (1991) provides a clear and lucid presentation of the assumptions and derivation of this approach. The entire summation in parentheses of equation (3.7) is the overall *selection gradient* on the phenotype—this is the dynamical descriptor of phenotypic selection. This quantity defines the overall strength and direction of natural selection on the average phenotype. Each term in this summation is the selection gradient associated with each fitness component of the species, which defines the strength and direction of phenotypic selection impinging on each.

Equation (3.7) can be used to describe changes in the trait caused by either adaptive evolution across generations of a population or the adaptive plasticity of individuals (i.e., individuals modify their phenotype in response to environmental conditions) within a generation. For adaptive evolution, V_{z_i} represents the additive genetic variation in z_i and defines the rate of the genetic response to phenotypic

selection, and its value is set to a small value (Lande 1982, Abrams et al. 1993). For adaptive plasticity, V_{z_i} is set to a large value, so that trait changes occur very quickly, or assumes a more complex functional form (Abrams et al. 1993). Thus, this framework can be used to explore both trait-mediated indirect effects of species interactions via adaptive plasticity (Werner and Peacor 2003, Křivan and Schmitz 2004, Ohgushi et al. 2013) and adaptive evolution (Lande 1982, Iwasa et al. 1991). The results are typically much the same.

Interpreted as a model of adaptive evolution, as I do here, equation (3.7) is simply a continuous time version of the standard breeders' equation describing the change in a quantitative trait due to natural or artificial selection (Lande 1979, Lande and Arnold 1983, Arnold and Wade 1984b, Lande 2007). Obviously, this derivation ignores within-population variation in phenotypes (e.g., Slatkin 1980, Taper and Case 1985, Price and Kirkpatrick 2009, Schreiber et al. 2011), and assumes that the dynamics of the mean trait value is a good approximation for the dynamics of evolution by natural selection (Lande 1982, 2007). Equation (3.7) can be extended to multivariate phenotypes (Lande 1982) and complex life cycles (Barfield et al. 2011), but for my purposes here, the main points can be made by considering only one trait per species with a simple life cycle. I will leave it to the reader and to future analyses to explore more complicated phenotypes and life histories in the contexts I explore here.

Equation (3.7) also identifies another key feature of the dynamics of natural selection that is little appreciated in the general literature—namely, the dynamical equilibria of natural selection (the peaks and nadirs of the fitness surface) also depend on the relative strengths of selection gradients operating separately on the various fitness components for each species. Each term in the summation in equation (3.7) describes how the contribution of that fitness component changes with a modification in the traits and abundances of all the species in the community; the magnitude of the selection gradient associated with a fitness component is the measure of the *strength of selection* on that same fitness component. This implies that the phenotypic trait value that is favored by selection overall will be more influenced by fitness components that experience stronger selection (McPeek 1996a). At an evolutionary equilibrium, whether it is stable or unstable, the various selection gradients must balance, and hence the selection strengths on the various fitness components weighted by the abundances of the interacting species must sum to zero (i.e., the terms in parentheses of equation (3.7) must sum to zero).

This framework also highlights that the members of a community evolve in a coevolutionary context that depends on both the abundance dynamics and trait dynamics of the interacting species. In a theoretical context, the entire system may reach a point equilibrium where all abundances and traits approach a single point in multidimensional abundance–trait space. At this point, each species will have a mean phenotype that gives $\partial W_i / \partial z_i = 0$ as either a fitness maximum or

fitness minimum on its adaptive surface that balances the contributions of the various fitness components to overall fitness (Abrams et al. 1993, Abrams and Matsuda 1997a). Our usual notion that natural selection moves populations uphill on the fitness surface implies a fitness maximum, but frequency-dependent selection generated by species interactions can cause stable fitness minima in some cases. Abrams et al. (1993) have illustrated the conditions where a stable fitness minimum for a species will result. A system may also express stable limit cycles in which both population abundances and trait values fluctuate through time (Abrams and Matsuda 1997b, Yoshida et al. 2003), as I will illustrate below.

As we will see, this framework clearly exposes the underlying drivers of the *ecological dynamics of natural selection*. The average fitness of the population changes as the mean trait value in the population alters, but average fitness also changes because the species' abundance as well as the traits and abundances of all the species with which it interacts also all change. Consequently, the fitness topography against which each species evolves may change continuously as species coevolve. Models that focus on genetic dynamics attempt to capture these fitness dynamics in formulations of density and frequency dependence, and various flavors of hard and soft selection (Levene 1953, Dempster 1955, Christiansen 1975, Nagylaki 1992, Charlesworth 1994). However, I think translating the processes to be considered here into those terms only obscures the ecological processes that produce natural selection. Previous analyses that utilize this more mechanistic approach to natural selection and coevolution have illustrated how fitness surfaces change as selection proceeds, but most have focused primarily on the evolutionary outcomes (e.g., Taper and Case 1985; Abrams et al. 1993; Abrams 2000; Abrams and Chen 2002; Abrams 2006; Price and Kirkpatrick 2009; Abrams and Fung 2010a, 2010b). In what follows, I will consider coevolution in many different types of community modules, and I will focus as much on the underlying causes of the ecological dynamics of natural selection as on the ultimate outcome.

Thus, the ecological opportunities available to species will change not only as the overall community structure changes through species additions and deletions (i.e., chapter 2), but also as the phenotypes and abundances of the species filling various community roles change. *An ecological opportunity represents both an ecological role to fill in a community and an evolutionary outcome of adapting to the community*.

TYPES OF TRAITS

The linkage between ecological and evolutionary dynamics is specified by how the traits of an individual interact with its environment to determine its overall fitness. Therefore, this framework also needs a mechanistic description of how

the traits of individuals influence the various components of their absolute fitness. Many phenotypic traits of an organism may simultaneously influence its survival, growth, and fecundity. Some traits may be almost universally important; body size comes to mind as one such trait. However, even body size is not so important in every facet of demography and life history for every species (Harmon et al. 2010). Because the ecologically important traits contribute to determining the absolute fitness of the organism, small changes in the value of any one would result in a change in overall fitness. Mathematically, this means that in equation (3.7), $\partial f_{ij}(z_i, \bar{z}_j)/\partial z_i \neq 0$ over much of the possible range of trait values. All aspects of the morphology, physiology, and behavior of an organism can potentially influence its demographic performance, and each ecologically important trait may influence absolute fitness through its simultaneous effects on multiple fitness components.

The effect of a phenotypic trait on a particular fitness component can take many functional forms, depending on the mechanism of the interactions between individuals and populations. However, all can be categorized by two general properties. The first is whether the fitness component changes in the same direction with changes in the trait over its entire range. If a phenotypic change in one direction increases a fitness component over the entire phenotypic range, I will refer to it as a *unidirectional* trait (following Abrams 2000). This trait is experiencing *directional selection* (i.e., $\partial f_{ij}(z_i, \bar{z}_j)/\partial z_i > 0$ or $\partial f_{ij}(z_i, z_j)/\partial z_i < 0$ for all z_i) for this fitness component over its entire phenotypic range, although the *strength of the selection gradient* (i.e., the magnitude of change in the fitness component with a unit change in the trait) may vary. Many different interactions are governed by unidirectional traits. For example, increasing the amount of time spent in its burrow should always decrease the probability of a rabbit being killed by a fox, and the more time spent hunting by the fox should increase the number of rabbits it catches. Escape speed is also a common example; if the prey can run or swim faster than the pursuing predator, the prey will have a greater chance of escape, but if the predator can run faster than the prey, the prey will likely be caught when attacked. Other examples are interactions in which the consumer is gape limited so that it cannot eat a resource above a certain size. Prey morphological defenses such as spines, slime, armor, and shells are also unidirectional traits in interactions with predators.

Alternatively, a trait may have a reversal in the directionality of change in some fitness component with trait change over different ranges of the phenotype; that is, $\partial f_{ij}(z_i, \bar{z}_j)/\partial z_i > 0$ over some phenotypic range, but $\partial f_{ij}(z_i, \bar{z}_j)/\partial z_i < 0$ over another range. Such a trait must, therefore, have either a fitness component maximum or minimum at some trait value (i.e., where $\partial f_{ij}(z_i, \bar{z}_j)/\partial z_i = 0$). Such traits have been termed *bidirectional*, because the fitness component increases with increasing trait values over one range but decreases with increasing trait value over another range (Abrams 2000). If the population's trait distribution includes

a fitness component maximum, the population experiences *stabilizing selection* from that component; whereas if the population's trait distribution includes a fitness component minimum, the population experiences *disruptive selection* from that component. If the population's trait distribution does not include the fitness maximum or minimum, it would experience directional selection. For example, consider a bird population feeding on the seeds of a plant that vary in size. Very small and very large seeds will have higher survival than seeds that closely match the sizes that are best manipulated and eaten using the bird's bill. The gill rakers of fish that are used to strain food particles from the water are also most efficient on a particular size of prey. In these cases, the consumer's feeding structure is most efficient on a particular size of resource, and the consumer is less efficient at feeding on resources that are both smaller and larger than this optimal size.

Traits also differ in whether their effect in determining the value of some fitness component does or does not depend on the trait value of another species; these are *dependent* or *independent* traits, respectively. For example, the contribution of swimming speed to determining a damselfly's survival under dragonfly predation cannot be determined without knowing how fast the dragonfly can strike and chase. Likewise, the contribution of size to determining a seed's survival under bird predation is unknown until one also knows the birds' bill sizes. These would both be dependent traits with respect to survival under predation. The contribution to determining the value of some fitness component by an independent trait does not depend on the trait values of other species. Increasing the time spend in a burrow will proportionally increase a rabbit's survival to a similar degree, regardless of the fox's phenotype. This does not mean that the fox's phenotype will have no influence on the rabbit's survival; it only means that the contributions of the rabbit and fox phenotypes to the rabbit's survival can be conceptually and mathematically partitioned in this trait. For dependent traits, this conceptual and mathematical partitioning cannot be done, because the contribution to the fitness component depends on the difference or ratio of the phenotypes of the interacting species (when measured on appropriate scales). Thus, we might expect frequency-dependent selection to be much more likely when dependent traits underlie a species interaction.

These categorizations highlight the dynamical nature of natural selection affecting the traits of interacting species. The relationship between fitness and the phenotype (i.e., the fitness surface as defined by equation (3.6)) is not a static feature of the environment, but rather has a dynamic that depends on both the abundances and traits of other interacting species. When dragonflies are rare, the fitness surface experienced by a damselfly population may have the same fundamental shape as when dragonflies are common; however, the height of the surface will be different in these two cases, because the rate at which dragonflies are

attacking damselflies will change with dragonfly abundance. The rate at which fitness changes at a given difference in swimming speed (i.e., the strength of the selection gradient) will also increase with the number of foraging dragonflies. Additionally, the shape of the fitness surface will differ between damselfly populations that face slow versus fast dragonflies. The dynamics of this relationship drive *coevolution* between species; this occurs when an evolutionary response in one species changes the form and intensity of selection on its interaction partner and thereby causes an evolutionary response, which in turn changes the form and intensity of selection on the first species, and so on (Thompson 1994).

Any particular trait may also influence the values of multiple fitness components. Size may affect the survival of a seed in the face of predators, but seed size may also influence the probability that the resulting plant survives the seedling stage of its life history. Increasing speed to chase down fleeing prey may decrease other components of fitness in the dragonfly. These multiple fitness effects may produce *synergies* (change in the trait causes two fitness components to increase or decrease) or *trade-offs* (change in the trait causes one fitness component to increase and the other to decrease) among various fitness components as they contribute to determining the shape of the overall fitness surface (Arnold and Wade 1984b). Also, the categories in which a trait falls (i.e., independent or dependent, unidirectional, or bidirectional) will typically differ among the fitness components it influences. For example, seed size may be a bidirectional-dependent trait with respect to seed predation, but a unidirectional-independent trait with respect to seedling survival.

DYNAMICS OF NATURAL SELECTION IN A VERY SIMPLE COMMUNITY

With this conceptual framework completed, we now need to actualize the simultaneous dynamics of abundances and traits that result from species interactions. Here, the focus will be on the interactions among consumers and resources to build on the purely ecological analyses presented in chapter 2. Let us begin by considering the interaction between one resource and one consumer. Also, assume that only one trait is ecologically important for each species (z_R for the resource and z_N for the consumer), and these traits influence both their per capita birth and death rates. Furthermore, their coevolutionary dynamics result from the functional response of their interaction, which is influenced by the traits of both species simultaneously. These per capita birth and death rates for each species are the separate components of absolute fitness that will define their evolutionary dynamics.

Using the basic models developed in chapter 2 to describe their population dynamics, the absolute fitnesses of individuals with specified trait values for an interacting consumer and resource species, respectively, are

$$\begin{aligned} \ln(W_N(z_N)) &= \frac{dN_{z_N}}{Ndt} = \frac{ba(\bar{z}_R, z_N)R}{1+a(\bar{z}_R, z_N)hR} - f(z_N) - gN \\ \ln(W_R(z_R)) &= \frac{dR_{z_R}}{Rdt} = c(z_R) - dR - \frac{a(z_R, \bar{z}_N)N}{1+a(\bar{z}_R, \bar{z}_N)hR} \end{aligned}. \tag{3.8}$$

(Because only one species is present per trophic level, I will forego subscripts to identify species in this chapter.) In this formulation, the parameters of the model are functions of the traits. Note that the denominator of the resource's functional response is a function of the average trait values of both species; this is because the consumer species overall is satiated primarily by resource individuals with the average trait value. In contrast, the denominator of the consumer's functional response depends on the average trait value of the resource species but the actual trait value of the consumer individual; this is because a consumer individual's level of satiation is based on that individual's trait value (Abrams 2000). When evaluated at the current average trait value for each species, equations (3.8) govern the population dynamics of these species:

$$\begin{aligned} \frac{dN}{dt} &= N\left(\frac{ba(\bar{z}_R, \bar{z}_N)R}{1+a(\bar{z}_R, \bar{z}_N)hR} - f(\bar{z}_N) - gN\right) \\ \frac{dR}{dt} &= R\left(c(\bar{z}_R) - dR - \frac{a(\bar{z}_R, \bar{z}_N)N}{1+a(\bar{z}_R, \bar{z}_N)hR}\right) \end{aligned}. \tag{3.9}$$

Equations (3.9) also define the landscapes of average fitness against mean trait values and species abundances for these two species when expressed in their per capita forms (e.g., dN/Ndt). The equations governing trait dynamics are then given by substituting equations (3.8) into (3.7):

$$\begin{aligned} \frac{d\bar{z}_N}{dt} &= V_{z_N}\left(\left.\frac{\partial\left(\frac{ba(\bar{z}_R, z_N)R}{1+a(\bar{z}_R, z_N)hR}\right)}{\partial z_N}\right|_{z_N=\bar{z}_N} + \left.\frac{\partial(-f(z_N)-gN)}{\partial z_N}\right|_{z_N=\bar{z}_N}\right) \\ \frac{d\bar{z}_R}{dt} &= V_{z_R}\left(\left.\frac{\partial(c(z_R)-dR)}{\partial z_R}\right|_{z_R=\bar{z}_R} + \left.\frac{\partial\left(-\frac{a(z_R, \bar{z}_N)N}{1+a(\bar{z}_R, \bar{z}_N)hR}\right)}{\partial z_R}\right|_{z_R=\bar{z}_R}\right) \end{aligned}. \tag{3.10}$$

The first term in each equation is the strength of the selection gradient on the respective species' birth fitness components, and the second term in each equation

is the strength of the selection gradient on their death fitness components. These yield

$$\begin{aligned}\frac{d\bar{z}_N}{dt} &= V_{z_N}\left(\frac{bR\dfrac{\partial a(\bar{z}_R, z_N)}{\partial z_N}\bigg|_{z_N=\bar{z}_N}}{(1+a(\bar{z}_R, z_N)hR)^2} - \frac{\partial f(z_N)}{\partial z_N}\bigg|_{z_N=\bar{z}_N}\right)\\ \frac{d\bar{z}_R}{dt} &= V_{z_R}\left(\frac{\partial c(z_R)}{\partial z_R}\bigg|_{z_R=\bar{z}_R} + \frac{N\dfrac{\partial a(z_R, \bar{z}_N)}{\partial z_R}}{(1+a(\bar{z}_R, \bar{z}_N)hR)}\bigg|_{z_R=\bar{z}_R}\right).\end{aligned} \tag{3.11}$$

Given these equations governing changes in abundances and trait means, all that is left is to specify the functional forms for how the parameters in the model depend on the traits of the species. As intuition would suggest, the different categories of traits have somewhat different effects on abundance and trait dynamics and different capabilities for how species may respond to different types of interactions. Even within a trait category, many different functional forms may be appropriate for different types of traits influencing different fitness components. Moreover, traits may be tied to various combinations of fitness components in different ways. An exhaustive analysis of various trait combinations is impossible to present. Here, I focus on a smaller set of trait combinations and functional forms, highlighting the resulting differences between different trait types to illustrate the major features of adaptive evolution that occurs as a result of species interactions.

Throughout this analysis, I will assume the resource's intrinsic birth rate, $c(z_R)$, and the consumer's intrinsic death rate, $f(z_N)$, are bidirectional-independent traits (fig. 3.1*A* and *B*, respectively).

I will use a quadratic function for the intrinsic birth rate of the resource:

$$c(z_R) = c_0\,(1 - \gamma(z_R - \tilde{z}_R^c)^2). \tag{3.12}$$

In this equation, the resource's intrinsic per capita birth rate has a maximum value of c_0 at its intrinsic birth rate optimum of $z_R = \tilde{z}_R^c$ and declines with larger deviations of the trait value from this optimum (fig. 3.1*A*). The parameter γ mediates the underlying strength of selection on z_R due to the birth fitness component—the rate at which the intrinsic birth rate declines away from $\tilde{z}_R^c$ with change in z_R. Therefore, z_R experiences overall stabilizing selection from the birth fitness component, and the strength of this stabilizing selection increases with increasing γ.

In analogous fashion, the intrinsic per capita death rate of the consumer is assumed to follow a quadratic function,

$$f(z_N) = f_0\left(1 + \theta(z_N - \tilde{z}_N^f)^2\right), \tag{3.13}$$

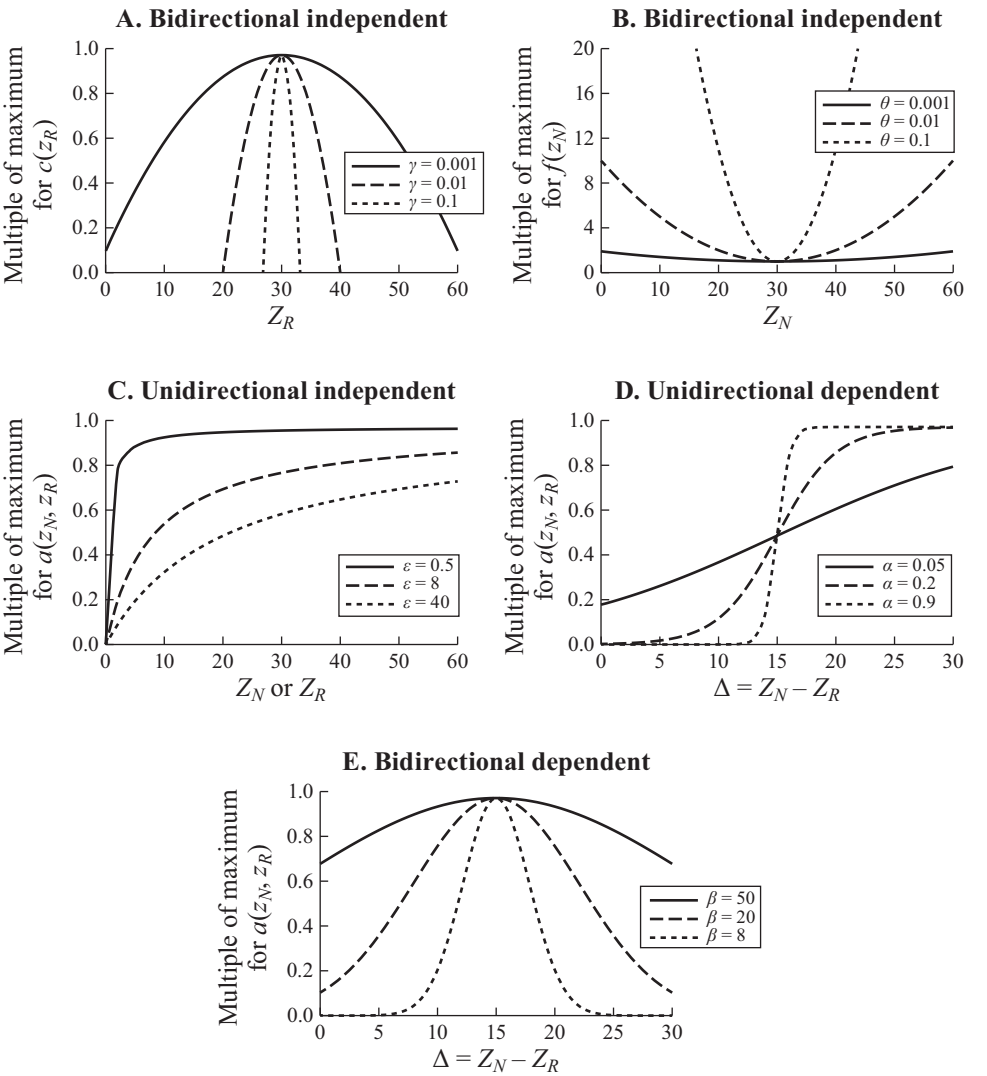

FIGURE 3.1. Functional forms used for the relationships between species trait values and parameters in the models. In each panel, the shape of the function for three different values of the tuning parameter that defines the underlying selection strength is shown. The functions are for the following trait types: (*A*) bidirectional-independent trait used for the resource intrinsic birth rate, (*B*) bidirectional-independent trait used for the consumer and predator intrinsic death rates, (*C*) unidirectional-independent traits defining the attack coefficients, (*D*) unidirectional-dependent traits defining the attack coefficient, and (*E*) bidirectional-dependent traits defining the attack coefficients.

where $z_N = \tilde{z}_N^f$ is the phenotype that minimizes the consumer's intrinsic death rate (i.e., its intrinsic death rate optimum), f_0 is the value at this minimum, and θ mediates the underlying strength of selection on z_N due to the death fitness component—the rate at which predator death rate increases away from $\tilde{z}_N^f$ with change in z_N (fig. 3.1*B*). Therefore, z_N also experiences stabilizing selection from the death fitness component and the strength of stabilizing selection increases with increasing θ.

The attack coefficient describing the per capita rate at which the consumer kills resource individuals is what generates the coevolutionary dynamics in this model. The attack coefficient can assume any of the various types of traits, depending on the specific traits involved in the consumer-resource interaction. In this analysis I consider three of the possible types. I neglect bidirectional-independent traits as a basis for the attack coefficient because trade-offs among fitness components cause the attack coefficient to rarely settle at the optimal value for the attack coefficient, and so the dynamics are in the end quite comparable to unidirectional-independent traits. Therefore, in the independent category, I present results only for unidirectional-independent traits defining attack coefficients.

First, many traits of interacting species have unidirectional-independent effects on their fitnesses and thus on the parameters in the model, and they can take myriad functional forms. For the analyses discussed here, imagine that z_R is a trait such as prey activity that affects the resource's exposure or conspicuousness to its consumers, and z_N is also a trait such as activity in which greater movement in the consumer increases its exposure to resources. Furthermore, assume that the attack coefficient is zero when $z_R = z_N = 0$ and increases asymptotically to a maximum value of a_0 as z_R and z_N increase. An equation with this general form is the Michaelis-Menten equation (Michaelis and Menten 1913),

$$a(z_R, z_N) = a_0 \frac{z_R}{(\varepsilon_R + z_R)} \frac{z_N}{(\varepsilon_N + z_N)}, \tag{3.14}$$

where a_0 is the asymptotic maximum, $z_R/(\varepsilon_R + z_R)$ is the independent effect that the resource trait has on the attack coefficient, and $z_N/(\varepsilon_N + z_N)$ is the independent effect of the consumer's trait on the attack coefficient (fig. 3.1*C*). The parameter ε_R is the underlying strength of selection on the attack coefficient via how fast the attack rate increases with z_R; ε_N does the same for z_N (fig. 3.1*C*).

When the consumer–resource interaction is influenced by traits such as evasion speed in the resource and pursuit speed in the consumer, the resource and consumer have unidirectional-dependent traits as their effects on the attack coefficient. Traits such as these are unidirectional because changes in only one direction increase the fitness contribution of this component for each species, but the difference between the trait values of the interacting species determine the fitness contribution to each. To model this type of trait combination determining the

attack coefficient, the difference between the consumer and resource trait values are $\Delta = z_N - z_R$, and I use a logistic function to describe the attack coefficient

$$a(z_R, z_N) = \frac{a_0}{1 + e^{-\alpha\Delta}}, \tag{3.15}$$

where a_0 is again the asymptotic maximum and α defines the steepness of the transition from low to high values around $\Delta = 0$ (fig. 3.1*D*). In the case of pursuit and evasion speeds, if the resource can run much faster than the consumer, Δ will be a large negative number, and so the attack coefficient will be near zero. In contrast, if the consumer can run substantially faster than the resource, Δ will be a large positive number, and the attack coefficient will be near a_0. For such traits, this interaction will continually apply directional selection for larger trait values to the death fitness component of the resource and to the birth fitness component of the consumer, and the strength of selection will increase with increasing α.

Finally, consider the consumer-resource interaction when the attack coefficient is influenced by *bidirectional-dependent* traits, such as bird bill size and seed size. In this case, the maximal attack coefficient occurs when the traits exactly match one another to give $\Delta = 0$ (when measured on appropriate scales), and declines away from this point in both directions. I use a Gaussian function to model the attack coefficient for these traits of

$$a(z_R, z_N) = a_0 e^{-\left(\frac{\Delta}{\beta}\right)^2}, \tag{3.16}$$

where a_0 is again the maximum, and β controls the steepness of decline away from $\Delta = 0$ in both directions (i.e., the strength of selection around $\Delta = 0$); see figure 3.1*E*. The attack coefficient will be near zero if the resource trait is very large or very small relative to the consumer trait (i.e., $|\Delta| \gg 0$), and will be near a_0 when the traits of the two species closely match (i.e., $\Delta \approx 0$). The form of selection experienced by the traits will also differ depending on the magnitude of the difference between them. When the species are similar (i.e., $\Delta \approx 0$), the consumer trait will experience stabilizing selection on its birth fitness component, and the resource trait will experience disruptive selection on its death fitness component. However, if the difference in trait values of the two species is large, they will experience directional selection in the same direction from this interaction on their respective fitness components.

The isoclines for R, N, $\bar{z}_R$, and $\bar{z}_N$ are complicated functions of population abundances and trait values, and so analytical solutions to the various models considered here are not possible. The following results are, therefore, based on extensive numerical simulations. The Matlab® code used for these simulations is available at http://enallagma.com/EvolutionaryCommunityEcology.

Throughout, I will illustrate the underlying mechanics of these models in features that are familiar to empirical ecologists and evolutionary biologists—namely. isoclines in phase portraits that drive abundance dynamics (e.g., fig. 2.2), and fitness surfaces that illustrate the relationship between fitness and phenotype. I do not intend this presentation as an exhaustive exploration of parameter space, but rather I will highlight the key dynamics and the drivers of those dynamics to expose the importance of the interplay between ecological and evolutionary dynamics.

I hope those who are interested in mutualisms will forgive me if I do not explicitly consider the evolution of mutualistic interactions here. Because of the length of this presentation, I am unable to consider that here. However, as I hope chapter 2 illustrated, many mutualistic interactions are really no different than consumer-resource interactions in understanding the properties of invasibility and coexistence. Preliminary analyses indicate that this is true for their evolution as well. I look forward to future analyses of the evolution of mutualisms with explicit trait mechanisms included.

THE DYNAMICS OF COEVOLUTION

When only one resource and one consumer are interacting, the fundamentals of coevolutionary dynamics are similar for all types of traits—independent or dependent, unidirectional or bidirectional—that define the nature of their interaction. Therefore, I will expound the central features of coevolution in this simplest of communities with a bidirectional-dependent trait defining the attack coefficient, as described by equation (3.16). The joint ecological and evolutionary dynamics of the system are then given by the following set of equations:

$$\begin{aligned}
\frac{dN}{dt} &= N\left(\frac{ba_0 e^{-\left(\frac{\bar{\Delta}}{\beta}\right)^2} R}{1+a_0 e^{-\left(\frac{\bar{\Delta}}{\beta}\right)^2} hR} - f_0\left(1+\theta(\bar{z}_N-\tilde{z}_N^f)^2\right) - gN\right)\\
\frac{dR}{dt} &= R\left(c_0\left(1-\gamma(\bar{z}_R-\tilde{z}_R^c)^2\right) - dR - \frac{a_0 e^{-\left(\frac{\bar{\Delta}}{\beta}\right)^2} N}{1+a_0 e^{-\left(\frac{\bar{\Delta}}{\beta}\right)^2} hR}\right)\\
\frac{d\bar{z}_N}{dt} &= V_{z_N}\left(-\frac{2ba_0\bar{\Delta}e^{-\left(\frac{\bar{\Delta}}{\beta}\right)^2} R}{\beta^2\left(1+a_0 e^{-\left(\frac{\bar{\Delta}}{\beta}\right)^2} hR\right)^2} - 2f_0\theta(\bar{z}_N-\tilde{z}_N^f)\right)\\
\frac{d\bar{z}_R}{dt} &= V_{z_R}\left(-2c_0\gamma(\bar{z}_R-\tilde{z}_R^c) - \frac{2a_0\bar{\Delta}e^{-\left(\frac{\bar{\Delta}}{\beta}\right)^2} N}{\beta^2\left(1+a_0 e^{-\left(\frac{\bar{\Delta}}{\beta}\right)^2} hR\right)}\right)
\end{aligned}. \qquad (3.17)$$

This system is too complex to evaluate analytically. The results presented below summarize a thorough exploration of parameter space using numerical simulations.

To develop deeper insights on the interplay between ecological and evolutionary dynamics, first consider the following very simple case. Imagine an island inhabited by a plant species (resource), and a seed-eating bird species (consumer, perhaps a Darwin's finch) invades and feeds on this plant's seeds. Initially, the resource species is adapted to a community lacking the consumer (i.e., it begins with its phenotype at its intrinsic birth optimum, which is $\tilde{z}_R^c = 10.0$ in this case) and is at its demographic equilibrium abundance for this trait value (i.e., $R^* = c(\tilde{z}_R^c)/d = 50$ for the parameters considered). Then the consumer invades this community at low abundance, and both species respond demographically and evolutionarily to one another. The consumer can only invade and establish in the community if it can initially increase in abundance or adapt sufficiently to have a positive population growth rate before it goes extinct. In the scenario considered here, the consumer has a positive population growth rate when it invades, and both species evolve to a stable equilibrium for both abundances and traits (figs. 3.2 and 3.3). (I will return to the second scenario when I discuss speciation in chapter 4.) An animation of the changes in selection on the various fitness components and overall fitness for both species is provided at http://press.princeton.edu/titles/11175.html; figure 3.3 presents snapshots from this animation.

At the start, the resource experiences no selection pressure from the consumer because the consumer's abundance is too low: the resource's death fitness component experiences no selection gradient imposed by the consumer, and so the shape of its overall fitness topography is completely defined by the shape of the fitness topography of its birth fitness component (fig. 3.3*A*). Thus, initially the resource does not evolve, because the consumer's abundance is too low to inflict enough mortality to impose phenotypic selection on the resource. In contrast, the consumer immediately begins to evolve a higher trait value because of the selection gradient associated with its birth fitness component from eating resource individuals (fig. 3.3.*B*); this causes the attack coefficient to increase, because this decreases the difference in the trait values (i.e., $\bar{\Delta} = \bar{z}_N - \bar{z}_R$) between the two species (i.e., to the left of the leftmost vertical dashed line in fig. 3.2*C*).

The resource only begins to evolve a higher trait value when the consumer's abundance increases to a level that inflicts substantial mortality (i.e., it creates a significant selection gradient on the resource's death fitness component, as shown in fig. 3.3*B*) and thus causes the resource's abundance to begin to decline (i.e., at the leftmost vertical dashed line in fig. 3.2*A*). At this point, the resource evolves rapidly to diverge from the consumer, which causes the former's intrinsic birth rate to decrease and the realized attack coefficient to also decrease rapidly (i.e., between the two vertical dashed lines in fig. 3.2*C*). The resource's abundance

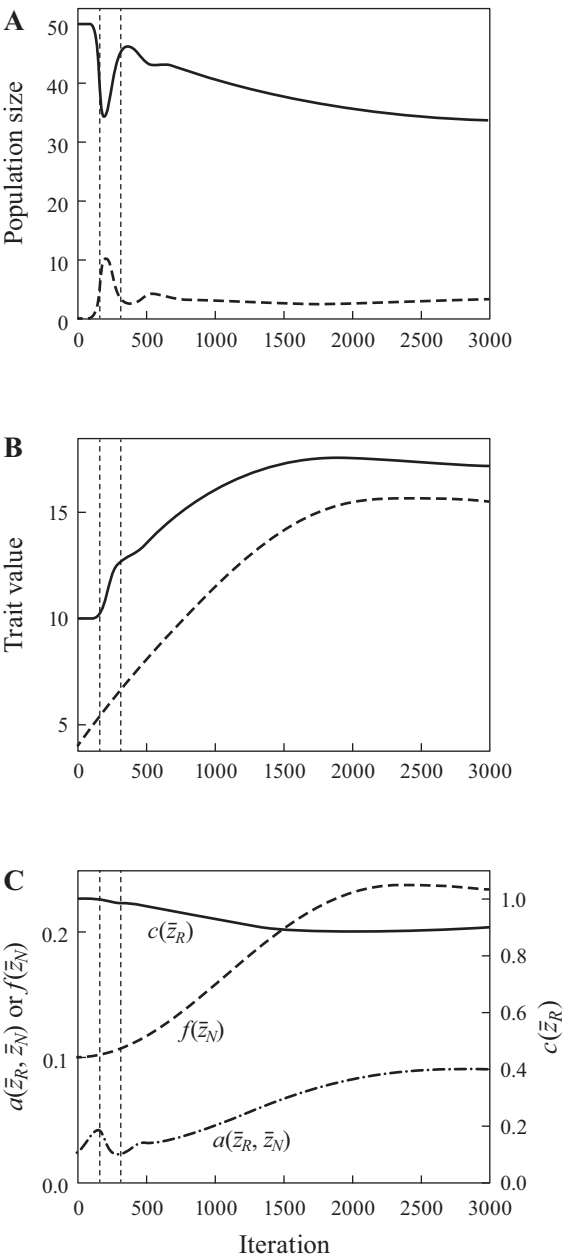

rebounds once its own evolution causes the realized attack coefficient to decrease sufficiently relative to its intrinsic birth rate.

Once this rapid phase of divergence is complete (i.e., the right vertical dashed line in fig. 3.2), the resource's and consumer's trait values continue to increase at a decelerating rate until they reach a stable equilibrium point in both abundances and trait values. Their evolution causes the resource's realized intrinsic birth rate $(c(\bar{z}_R))$ to decline, because the resource evolves away from its intrinsic birth optimum $(\tilde{z}_R^c)$, and also causes the consumer's realized intrinsic death rate $(f(\bar{z}_N))$ to increase, because the consumer evolves away from its intrinsic birth optimum $(\tilde{z}_N^f)$ (fig. 3.2*C*). The attack coefficient $(a(\bar{z}_R, \bar{z}_N))$ also increases as a result of this coevolution because the difference between the consumer's and resource's trait values decreases (fig. 3.2*C*). The positions of the abundance isoclines change as the realized parameters of the system evolve (fig. 3.2*C*), and the system eventually has abundance isoclines as in figure 2.2*F* at this stable equilibrium.

At the equilibrium, the consumer is at a local fitness maximum, but in this case the resource is at a local fitness minimum (fig. 3.3*C*). Because both species are at their demographic equilibria, the values of the overall fitness curves at the average phenotypes are both zero (remember that in this modeling framework, average fitness is measured on a log scale; fig. 3.3*C*) because their birth and death fitness components are equal in magnitude but opposite in sign (i.e., the values of the fitness component curves at the average phenotype sum to zero for each species; fig. 3.3*C*). In addition, each species is at an overall fitness optimum because the selection gradients on their underlying fitness components balance. The resource experiences directional selection for decreasing its trait value due to selection on its birth fitness component, but this is balanced by directional selection of the same magnitude to increase its trait value via its death fitness component (fig. 3.3*C*). Likewise, the consumer experiences directional selection for increasing its trait value due to selection on its birth fitness component, but this is balanced by directional selection of the same magnitude to decrease its trait value due to selection on its death fitness component (fig. 3.3*C*).

FIGURE 3.2. Abundance and trait dynamics of a consumer-resource coevolution. In this example, the resource is initially adapted to an environment lacking the consumer, and the consumer is then introduced at low abundance. The panels show the dynamics of (*A*) population sizes, (*B*) trait values, and (*C*) realized values of the attack coefficient (*a*, *dot-dash line*), resource intrinsic birth rate (*c*, *solid line*) and consumer intrinsic death rate (*f*, *dashed line*). In panels *A* and *B*, the *solid lines* identify the resource values, and the *dashed lines* identify the consumer values. The parameters used for this example are $c_0 = 1.0$, $d = 0.02$, $a_0 = 0.1$, $b = 0.1$, $h = 0.1$, $f_0 = 0.1$, $g = 0.0$, $\beta = 5.0$, $\gamma = 0.002$, $\theta = 0.01$, $\tilde{z}_R^c = 10.0$, $\tilde{z}_N^f = 4.0$, and $V_{z_R} = V_{z_N} = 0.2$. (This figure is redrawn from figure 2 of McPeek 2017, with permission.)

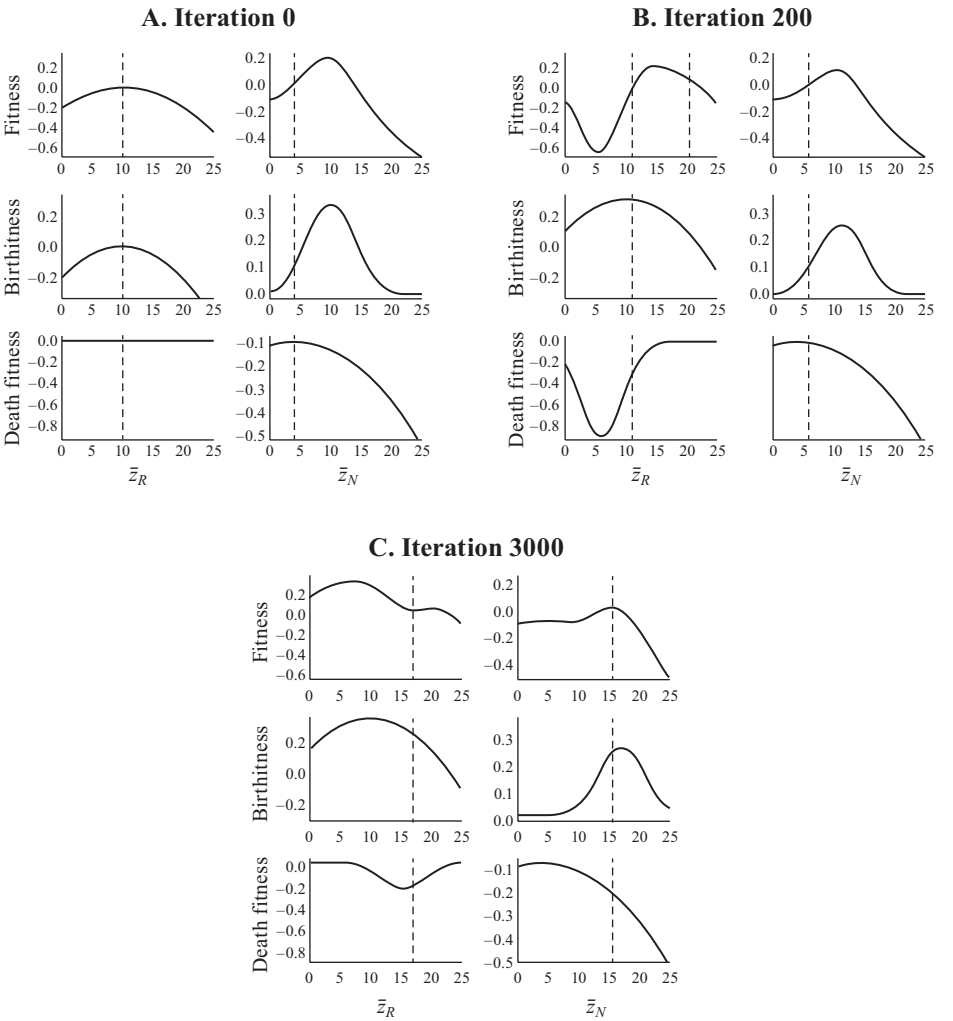

FIGURE 3.3. Fitness surfaces for the resource and consumer at various points in the scenario illustrated in figure 3.2. The final equilibrium for the example is given in figure 3.2. The groups of panels show the overall fitness surface, and the birth and death fitness component surfaces, for each species at iterations (*A*) 0, (*B*) 200, and (*C*) 3000. The *vertical dashed lines* in each panel identify the trait value of that species at that point. Note that the consumer is at a stable fitness maximum and the resource is at a stable fitness minimum at the equilibrium in iteration 3000. The parameters are given in figure 3.2. (This figure is redrawn from figure 2 of McPeek 2017, with permission.)

The resource is maintained at this local fitness minimum because if its average trait value moves in either direction, changes in the consumer's abundance will alter the selection gradient on the resource's death fitness component to move it back to this trait optimum (see also Abrams et al. 1993, Abrams and Matsuda 1997a). If the resource's trait mean is perturbed to a lower value away from this equilibrium, the consumer's abundance immediately increases because of the resulting increase in the attack coefficient, which increases the steepness of the selection gradient associated with the resource's death fitness component from predation; this then alters the shape of the resource's overall fitness surface to increase its trait value. In contrast, if the resource's trait mean is perturbed to a higher value, the consumer's abundance immediately decreases because of the resulting decrease in the attack coefficient, which reduces the steepness of the selection gradient on the resource's death fitness component, and thus changes the shape of the resource's overall fitness surface to decrease its trait value. Although the resource is experiencing disruptive selection at this minimum fitness optimum, any evolutionary response by the resource away from this equilibrium will alter its overall fitness surface to bring the population back to the equilibrium due to the ecological response of consumer abundance. Likewise, opposing directional selection pressures impinging on the consumer's various fitness components maintain it at its fitness optimum (fig. 3.3*C*).

Remember that the selection gradient associated with a fitness component is the slope of the line tangent to the fitness surface at the average phenotype. Thus, the slopes of the tangent lines on the birth and death fitness components (i.e., the terms inside the parentheses in equation (3.10)) are equal in magnitude and opposite in sign for each species at this evolutionary equilibrium. In this case, as probably in most cases in nature, a fitness optimum on the overall fitness surface results from a balancing of various underlying fitness components (Travis 1989). Also, note in equations (3.17) that the selection gradient of the resource's death fitness component depends on the abundance and average trait value of the consumer, and the selection gradient of the consumer's birth fitness component depends on the abundance and average trait value of the resource. *The fitness components of each species change in response to abundance and trait changes in the other species, and both the various fitness components and the various selection gradients must balance in each species at the demographic and evolutionary equilibrium.*

Throughout the course of this coevolution, the fitness surfaces for the two species are not static—their shapes change because of changes in both abundances and traits—and the traits of the two species closely follow the changing positions of the optimal phenotypes on the overall fitness surfaces (fig. 3.3; see also the animation of the fitness component surfaces in this figure at http://press.princeton.edu/titles/11175.html). Changes in the optimal phenotype for both

species are driven by how changes in their abundances and traits determine the mortality inflicted on the resource by the consumer (the resource's death fitness component) and how this mortality translates into consumer births (the consumer's birth fitness component). Also, the same phenotype ($\tilde{z}_R^c$) gives the highest birth fitness component value to the resource throughout, but the fitness value at this fitness component optimum changes because of density dependence in birth rate, and the same is true for the death fitness component of the consumer.

Trait Cycling

Another interesting situation that illuminates the ecological drivers of trait evolution is when the entire system enters a stable limit cycle or chaotic cycle in which both abundances and traits change continuously over time (Hochberg and Holt 1995, Abrams and Matsuda 1997b, Abrams 2000, Yoshida et al. 2003). Such a situation is illustrated in figure 3.4 when bidirectional-dependent traits define the attack coefficient. Trait cycling occurs in areas of parameter space with a number of specific features: the resource's maximum intrinsic birth rate (c_0) and the maximum attack coefficient (a_0) are relatively high, the underlying strengths of selection gradients on the resource's intrinsic birth rate (γ) and consumer's intrinsic death rate (θ) are weak relative to the underlying selection strength on the attack coefficient (β), and the handling time of the consumer (h) is zero or relatively low. In other words, cycling occurs when the interaction is a greater determinant of the shape of the overall fitness surfaces of both species relative to other selection pressures, and when the demographic response of the consumer is not substantially damped by satiation when the resources are abundant.

In contrast to trait cycling, the species' abundances cycle in areas of parameter space where the abundance isoclines cross in ways that cause dynamic instability (see chapter 2). These areas of parameter space are generally characterized by the consumer having such a high handling time that the consumer isocline crosses the resource isocline to the left of its apex (Rosenzweig and MacArthur 1963, Rosenzweig 1969), or by particular community module configurations (Holt and Polis 1997, Křivan and Diehl 2005, Tanabe and Namba 2005). The species' traits may evolve into areas where abundance limit cycles occur, but once there the traits do not evolve appreciably. Consequently, the cycles are driven exclusively by the dynamical properties of abundance regulation given the traits of the interacting species and the resulting parameters.

Conversely, if traits cycle, abundances always cycle as well. The dynamics of this system is governed by a set of four isoclines in the four-dimensional joint abundance/trait space of equation (3.17). The shapes of the four isoclines near

where they cross to form a local equilibrium is what fosters the cycling. Because the trajectory of the cycle causes the system's position to change on all four axes at once, the abundance isoclines (e.g., fig. 2.2) appear to change shape when considered in isolation, as do the trait isoclines. The trait isoclines have interesting shapes, but because we almost exclusively consider the dynamics of evolution in the context of the shapes of the fitness surfaces, I will not consider the trait isocline shapes here.

When trait cycling occurs with bidirectional-dependent traits defining the attack coefficient, the resource continually cycles through evolving away from the consumer and then evolving toward the consumer, while the consumer continually chases the resource in trait space (fig. 3.4*B*). This coevolutionary chase can be understood by the continual changes in the two species' fitness surfaces (fig. 3.4*D–G*). As a result, their abundances also cycle (fig. 3.4*A*) because the realized demographic parameters are continually changing (fig. 3.4*C*). (In this description, I will focus on the evolutionary aspects of the cycle. I will leave it for the reader to discern how this evolution drives the population dynamics seen in figure 3.4*A*.)

The most important evolutionary insights are made by considering selection associated with the various fitness components of the two species through one of these trait cycles. Figure 3.4*D–G* shows the fitness surfaces for the two species at four different points in the trait cycle. (An animation of figure 3.4 is also available at http://press.princeton.edu/titles/11175.html.) At iteration 2500 (fig. 3.4*D*), the resource is near its maximum trait value in the cycle, and the consumer is evolving toward the resource (fig. *3.4B*). Here, the resource is very near the local adaptive peak in overall fitness at the high trait value because the strengths of the selection gradients on its birth and death fitness components are strong and nearly balance. Note that the resource's overall fitness surface at this point has a second adaptive peak that is substantially below its intrinsic birth optimum, and the bottom of the fitness valley between the two peaks is very near the consumer's trait value. At this point, the consumer continues to evolve toward the resource because the positive selection gradient on its birth fitness component is much higher than the negative selection gradient on its death fitness component.

As the consumer continues to evolve toward the resource (e.g., iteration 2650; fig. 3.4*E*), the height of the adaptive peak on which the resource resides declines to the point where this is no longer an adaptive peak at all. This is caused by the shift in the balance of selection gradients on the resource's birth and death fitness components. Here, a very interesting evolutionary dynamic has happening: as the consumer evolves toward the resource, the magnitude of the attack coefficient increases as a result, and thus the ecological interaction strength between them (the strength of the selection gradient on the resource's death fitness component

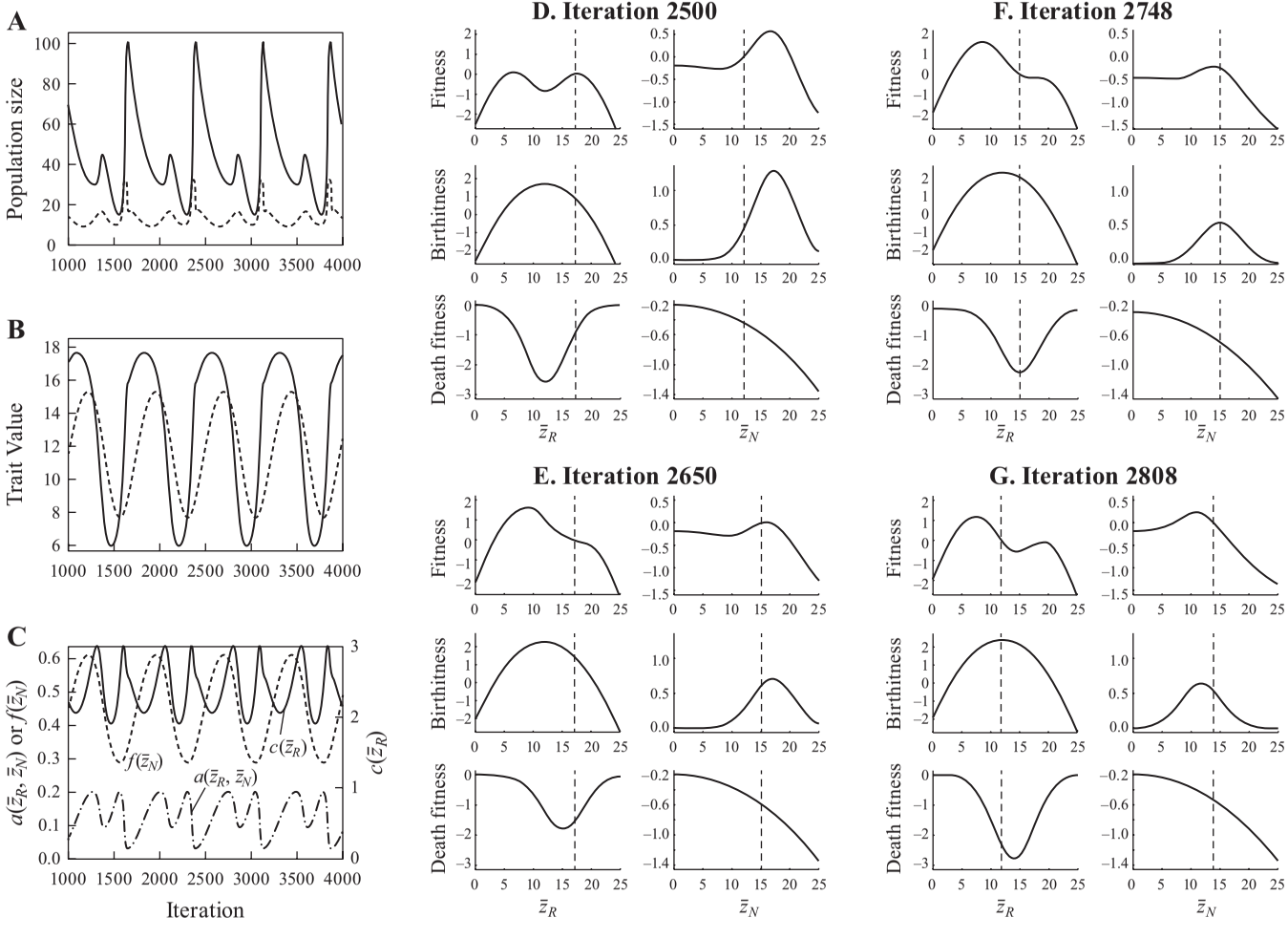

caused by predation from the consumer) actually decreases. Stronger selection now impinges on the resource's birth fitness component, and the fitness peak on which it resided has now disappeared. Consequently, the resource reverses its evolutionary course and begins to evolve toward the consumer, even though this increases the realized attack coefficient and the consumer's abundance still further, and so increases its death rate due to predation (fig. 3.4*C*).

At iteration 2748, the resource's and consumer's trait values match (fig. 3.4*F*). Now the selection gradients resulting from the interaction between the species are zero; even though the attack coefficient is at its maximum value and the consumer is at its maximal abundance, and so is imposing maximal death rate due to predation on the resource (see equation (3.16) and fig. 3.4*C*), no selection impinges on either species because of the trophic interaction between them. Overall selection to decrease the resource's mean trait value is due solely to the negative selection gradient to increase its intrinsic birth rate, and overall selection to decrease the consumer's mean trait value is due solely to the negative selection gradient to decrease its intrinsic death rate.

As the resource's mean trait value passes the consumer's, natural selection due to predation reappears and strengthens again on both species to decrease both their trait values, whereas the selection gradients on their respective intrinsic birth and death rates decrease in magnitude. At iteration 2808, the resource reaches its intrinsic birth optimum ($\tilde{z}_R^c$), and so its intrinsic birth rate is maximized (see equation (3.12) and fig. 3.4*C*), but the selection gradient on its birth fitness component is zero (fig. 3.4*G*). By this time, the resource's overall fitness surface again has two fitness peaks, but overall selection is now pushing the resource toward the lower peak. As the resource's trait value passes $\tilde{z}_R^c$ and continues to decrease, the selection gradient on its birth fitness component increases to pull it back toward $\tilde{z}_R^c$, and the selection gradient on its death fitness component decreases but remains larger than the birth selection gradient, which pushes the resource to lower trait values. As a result, the height of the fitness peak to which it is evolving begins to decline;

FIGURE 3.4. An example of trait cycling when bidirectional-dependent traits define the attack coefficient between the consumer and resource. The panels show the dynamics of (*A*) population sizes, (*B*) trait values, and (*C*) realized values of the attack coefficient (*a*, *dot-dash line*), resource intrinsic birth rate (*c*, *solid line*) and consumer intrinsic death rate (*f*, *dashed line*). In panels *A* and *B*, the *solid lines* identify the resource values, and the *dashed lines* identify the consumer values. Panels *D–G* show these overall fitness surfaces and the birth and death fitness component surfaces at specific iterations in the simulation. The parameters used for this example are $c_0 = 3.0$, $d = 0.02$, $a_0 = 0.2$, $b = 0.1$, $h = 0.0$, $f_0 = 0.2$, $g = 0.0$, $\beta = 5.0$, $\gamma = 0.01$, $\theta = 0.01$, $\tilde{z}_R^c = 12.0$, $\tilde{z}_N^f = 1.0$, and $V_{z_R} = V_{z_N} = 0.2$. (This figure is redrawn from figure 2 of McPeek 2017, with permission.)

it continues to decline as the consumer continues to evolve to chase the resource in phenotype space. The resource's trait value reaches its lowest value when the birth and death selection gradients again balance. At this point, the lower fitness peak has decreased in height to such a degree that it is no longer a peak (analogous but reversed to the overall fitness surface in iteration 2650), and overall selection then causes the resource's trait value to increase and again evolve toward that of the consumer. The other half of the trait cycle is then simply this entire series of relationships in reverse. Note that the resource evolves a more extreme phenotype than the consumer on both extremes of the cycle (fig. 3.4*B*).

With this cycling, the resource is undergoing continual shifts between two adaptive peaks, while the consumer is chasing a continuously moving single fitness peak (fig. 3.4 and http://press.princeton.edu/titles/11175.html). These peak shifts occur exclusively because of the dynamics of the overall fitness surfaces for the two species caused by the changing strengths of selection gradients associated with their various fitness components. The resource is cycling between extreme phenotypes that give it relatively low birth and death rates, but it must pass through a period of high birth and death rates to traverse from one to the other. The magnitudes of selection gradients on its two fitness components follow a countervailing cycle, both being steep at the trait extremes of the cycle and relatively shallow between.

When unidirectional-dependent traits define the attack coefficient, trait cycling occurs over a smaller total area of parameter space but under similar parameter relationships. Trait cycling in this case also takes a quite different form. For this situation, equation (3.15) is used for the attack coefficient in equations (3.9) and (3.10) to give

$$\begin{aligned}
\frac{dN}{dt} &= N\left(\frac{\dfrac{ba_0R}{1+e^{-\alpha\bar{\Delta}}}}{1+\dfrac{a_0hR}{1+e^{-\alpha\bar{\Delta}}}} - f_0\left(1+\theta(\bar{z}_N-\tilde{z}_N^f)^2\right) - gN\right)\\
\frac{dR}{dt} &= R\left(c_0\left(1-\gamma(\bar{z}_R-\tilde{z}_R^c)^2\right) - dR - \frac{\dfrac{a_0N}{1+e^{-\alpha\bar{\Delta}}}}{1+\dfrac{a_0hR}{1+e^{-\alpha\bar{\Delta}}}}\right)\\
\frac{d\bar{z}_N}{dt} &= V_{z_N}\left(\frac{ba_0\alpha e^{-\alpha\bar{\Delta}}R}{(1+e^{-\alpha\bar{\Delta}})^2\left(1+\dfrac{a_0hR}{1+e^{-\alpha\bar{\Delta}}}\right)^2} - 2f_0\theta(\bar{z}_N-\tilde{z}_N^f)\right)\\
\frac{d\bar{z}_R}{dt} &= V_{z_R}\left(-2c_0\gamma(\bar{z}_R-\tilde{z}_R^c) + \frac{2a_0\alpha e^{-\alpha\bar{\Delta}}N}{(1+e^{-\alpha\bar{\Delta}})\left(1+\dfrac{a_0hR}{1+e^{-\alpha\bar{\Delta}}}\right)}\right)
\end{aligned} \quad . \qquad (3.18)$$

Generally, when trait cycling occurs with unidirectional-dependent traits defining the interaction between the two species, the consumer evolves to have a higher trait value than the resource (fig. 3.5*B*). The resource is again undergoing shifts between two alternative adaptive peaks, and the consumer is chasing a single moving peak. (An animation of figure 3.5 is also available at http://press.princeton.edu/titles/11175.html.) For much of the cycle, the selection gradients on the resource's death fitness component and the consumer's birth fitness component are nearly zero because the consumer's trait value is much higher than the resource's trait value (fig. 3.5). This means that overall selection on the resource favors trait values very near its intrinsic birth optimum ($\tilde{z}_R^c$) (fig. 3.5*D*).

As the predator evolves lower trait values, the steep transition zone of change in the attack coefficient (fig. 3.1*D*) and thus in the resource's death fitness component moves toward the resource's trait value (fig. 3.5*D–E*). Once the consumer evolves to a low enough value to increase the selection gradient on the resource's death fitness component, the overall fitness peak on which the resource resides temporarily disappears in favor of higher trait values in the resource, and thus it rapidly transitions to the alternative adaptive peak (fig. 3.5*E*). This evolutionary response that decreases the attack coefficient causes a spike in the resource's abundance even though its intrinsic birth rate declines sharply (fig. 3.5*A–C*). The consumer then rapidly reverses its evolutionary course to evolve higher trait values due to the change in the selection gradient on its birth fitness component (fig. 3.5*E–F*). In addition, this response to selection in the consumer causes its abundance to decline because of the increase in its intrinsic death rate (fig. 3.5*A–C*). As the consumer evolves higher trait values, the selection gradient on the resource's birth fitness component transitions back to the flat part of the fitness component surface, and overall selection then favors the resource to evolve back toward the reformed lower adaptive peak in overall fitness near its intrinsic birth optimum (fig. 3.5*F–G*).

Although the resource is again shifting between alternative adaptive peaks, the two peaks in this case represent very different demographics. One fitness peak is very near its intrinsic birth optimum; the resource has its highest birth rate but also a high death rate at this peak, and the selection gradients on both fitness components are relatively weak. The other fitness peak is far from its intrinsic birth optimum; here it has its lowest birth rate and lowest death rate, but the selection gradients on both fitness components are steepest. Thus, trait cycling with unidirectional-dependent traits defining the attack coefficient moves the resource between two extreme phenotypes that represent a trade-off of fitness components. In contrast, remember that cycling with bidirectional-dependent traits defining the attack coefficient moves the resource between alternative phenotypes that both have low birth and death rates.

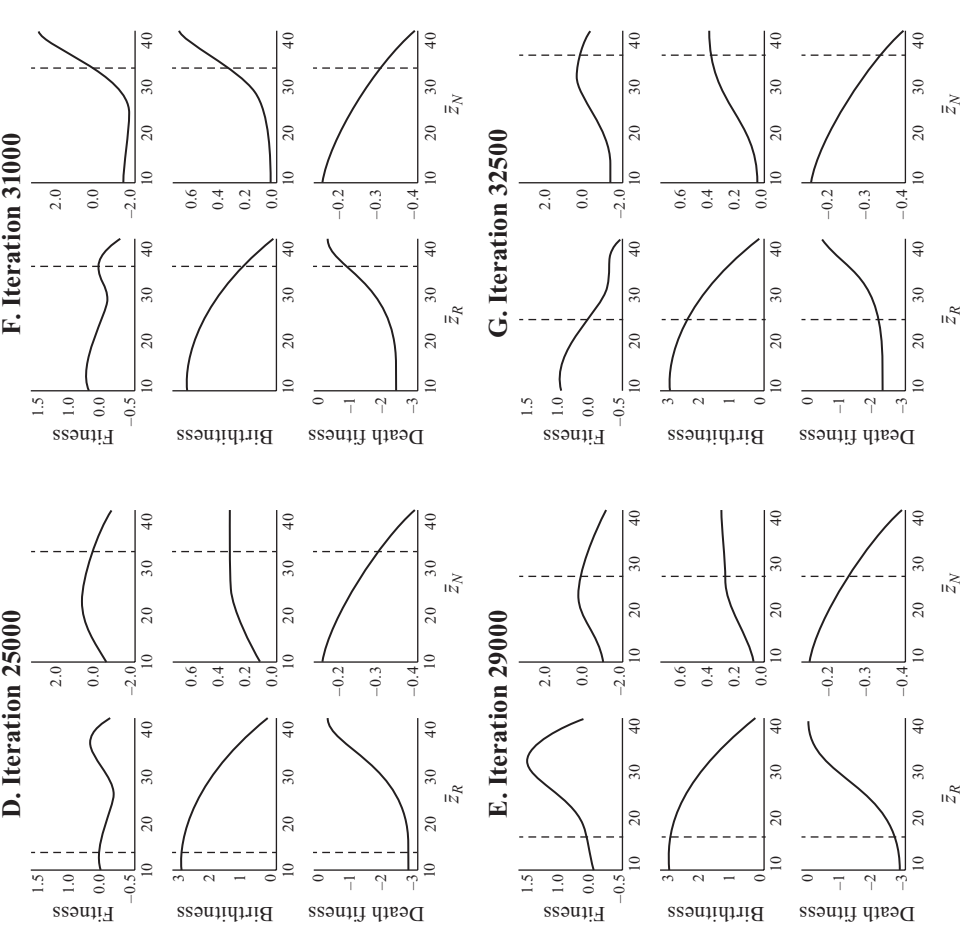

Trait cycling again typically occurs only in areas of parameter space where the underlying selection strengths on the resource's intrinsic birth rate and the consumer's intrinsic death rate are weak relative to the underlying selection strength on the attack coefficient (α). For example, in this case with unidirectional-dependent traits underlying the attack coefficient, trait cycling does not occur if the underlying selection strength on the attack coefficient is weak (i.e., small α) relative to the underlying selection strengths on the intrinsic resource birth rates (i.e., large γ) or the intrinsic consumer death rate (i.e., large θ) (cf. fig 3.6*A–C* to 3.6*D–F*). Likewise, if γ and θ are increased relative to α, cycling is also stopped (Fig. 3.6*G–I*). Note that in this latter case, the trait values favored by selection are closer to the intrinsic birth and death optima for the respective species than in the case where the attack coefficient is the weaker factor (cf. figs. 3.6*B* and *H*). However, if α is then increased again relative to γ and θ, trait cycling occurs again (fig. 3.6*J–L*).

If the traits of the two species have unidirectional-independent effects on the attack coefficient, as when defined by equation (3.14), trait cycling occurs only in a very narrow range of parameter space, and it occurs differently from dependent traits. Substituting equation (3.14) into equations (3.9) and (3.10) yields

$$\begin{aligned}
\frac{dN}{dt} &= N\left(\frac{\dfrac{ba_0\bar{z}_R\bar{z}_N R}{(\varepsilon_R+\bar{z}_R)(\varepsilon_N+\bar{z}_N)}}{1+\dfrac{a_0\bar{z}_R\bar{z}_N hR}{(\varepsilon_R+\bar{z}_R)(\varepsilon_N+\bar{z}_N)}} - f_0\left(1+\theta(\bar{z}_N-\tilde{z}_N^f)^2\right) - gN\right)\\
\frac{dR}{dt} &= R\left(c_0\left(1-\gamma(\bar{z}_R-\tilde{z}_R^c)^2\right) - dR - \frac{\dfrac{a_0\bar{z}_R\bar{z}_N N}{(\varepsilon_R+\bar{z}_R)(\varepsilon_N+\bar{z}_N)}}{1+\dfrac{a_0\bar{z}_R\bar{z}_N hR}{(\varepsilon_R+\bar{z}_R)(\varepsilon_N+\bar{z}_N)}}\right)\\
\frac{d\bar{z}_N}{dt} &= V_{z_N}\left(\frac{\dfrac{ba_0\varepsilon_N\bar{z}_R R}{(\varepsilon_R+\bar{z}_R)(\varepsilon_N+\bar{z}_N)^2}}{\left(1+\dfrac{a_0\bar{z}_R\bar{z}_N hR}{(\varepsilon_R+\bar{z}_R)(\varepsilon_N+\bar{z}_N)}\right)^2} - 2f_0\theta(\bar{z}_N-\tilde{z}_N^f)\right)\\
\frac{d\bar{z}_R}{dt} &= V_{z_R}\left(-2c_0\gamma(\bar{z}_R-\tilde{z}_R^c) + \frac{\dfrac{a_0\varepsilon_R\bar{z}_N N}{(\varepsilon_R+\bar{z}_R)^2(\varepsilon_N+\bar{z}_N)}}{1+\dfrac{a_0\bar{z}_R\bar{z}_N hR}{(\varepsilon_R+\bar{z}_R)(\varepsilon_N+\bar{z}_N)}}\right)
\end{aligned}. \qquad (3.19)$$

FIGURE 3.5. An example of trait cycling when unidirectional-dependent traits define the attack coefficient between the consumer and resource. The panels are as described in figure 3.4. The parameters used for this example are $c_0 = 3.0$, $d = 0.02$, $a_0 = 0.5$, $b = 0.1$, $h = 0.0$, $f_0 = 0.15$, $g = 0.0$, $\alpha = 0.25$, $\gamma = 0.001$, $\theta = 0.001$, $\tilde{z}_R^c = 12.0$, $\tilde{z}_N^f = 1.0$, and $V_{z_R} = V_{z_N} = 0.2$. (This figure is redrawn from figure 5 of McPeek 2017, with permission.)

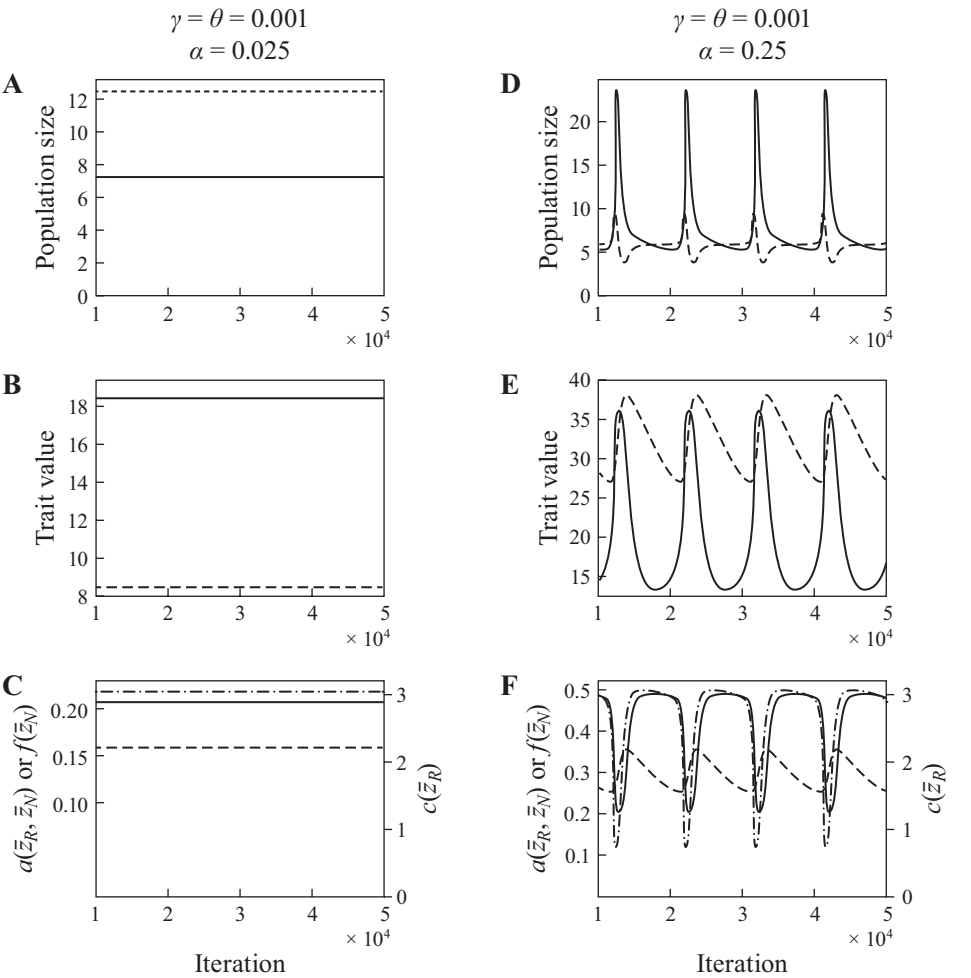

FIGURE 3.6. Examples illustrating that the relative selection strengths on the attack coefficient and the intrinsic resource birth and consumer death rates influence the prevalence of trait cycling. Each column of panels shows the results of a simulation with specific values for the parameters defining the underlying selection strengths on these three fitness components (specific values are given *above* each column). The *top row* of panels gives the dynamics of population sizes, and the *middle row* of panels gives the dynamics of the trait values. In these panels, the *solid lines*

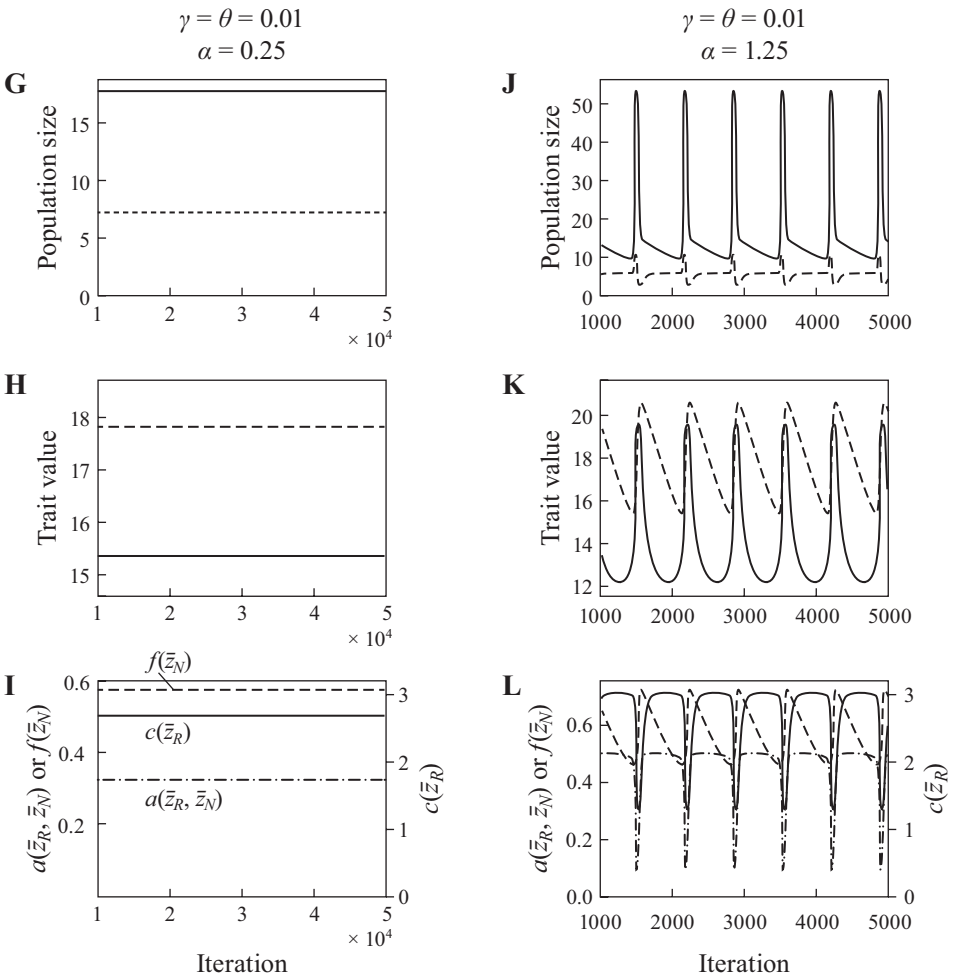

identify the resource values, and the *dashed lines* identify the consumer values. The *bottom row* of panels gives the dynamics of the realized values of the attack coefficient (*a*, *dot-dash* line), resource intrinsic birth rate (*c*, *solid* line), and consumer intrinsic death rate (*f*, *dashed* line). All other parameters are as given in figure 3.5. (This figure is redrawn from figure 6 of McPeek 2017, with permission.)

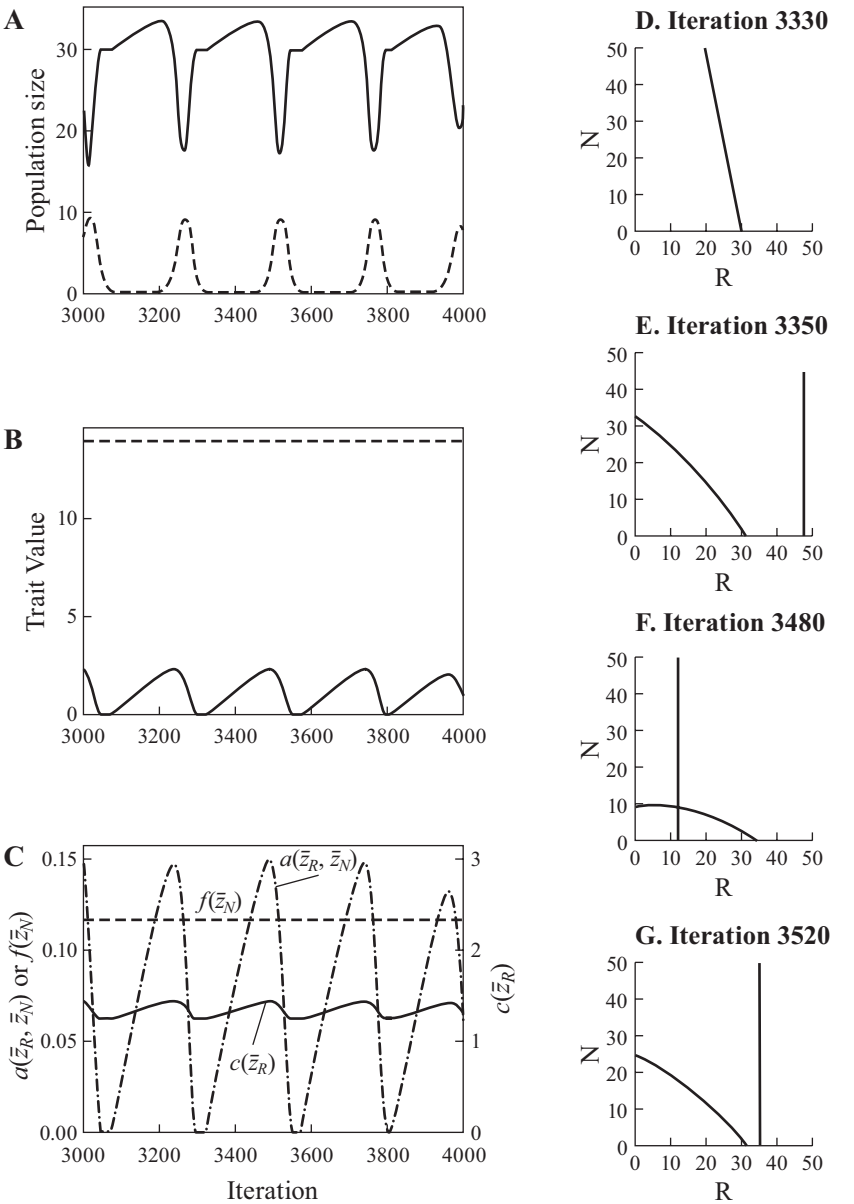

FIGURE 3.7. An example of trait cycling when unidirectional-independent traits define the attack coefficient between the consumer and resource. Panels *A–C* are as described in figure 3.4. Panels *D–G* show the abundance isoclines at specific iterations of the simulation. The parameters used for this example are $c_0 = 2.0$, $d = 0.04$, $a_0 = 3.5$, $b = 0.1$, $h = 0.3$, $f_0 = 0.1$, $g = 0.0$, $\varepsilon_R = 20.0$, $\varepsilon_N = 20.0$, $\gamma = 0.001$, $\theta = 0.001$, $\bar{z}_R^c = 20.0$, $\bar{z}_N^f = 1.0$, and $V_{z_R} = V_{z_N} = 0.2$.

The first striking difference in trait cycling when independent traits are involved is that only the trait of the resource cycles (fig. 3.7*B*). (An animation of figure 3.7 is also available at http://press.princeton.edu/titles/11175.html.) Moreover, what drives the resource's trait cycles is the cycling in the abundance of the consumer. However, the consumer's abundance cycles are caused by changes in the positions of the abundance isoclines due to the evolution of the resource, and not from inherent instability caused by the shapes of the abundance isoclines.

When the resource is at its lowest trait value in the cycle, the attack coefficient is at a minimum. In the cycling system depicted in figure 3.7, the minimum trait value of the resource in the cycle is zero, which in this case means the attack coefficient is zero. At this point in the cycle, with $a(\bar{z}_R, \bar{z}_N) = 0$ (fig. 3.7*C*), the resource's abundance isocline is parallel to the *N*-axis, and the consumer's abundance isocline is at $+\infty$ on the *R*-axis. Thus, the consumer is at that instant being driven extinct. As a result, the resource increases to its equilibrium abundance and evolves higher trait values to move toward its intrinsic birth optimum, because mortality from the consumer is very low. However, this increase in the resource's trait value increases the attack coefficient, which moves the consumer's isocline to lower values of the *R*-axis (fig. 3.7*E*). As the resource continues to evolve higher trait values, eventually the consumer's isocline moves to lower values on the *R*-axis so that it crosses the resource isocline, and the consumer then increases in abundance (fig. 3.7*F*). When the resource reaches its maximum trait value in the cycle, the attack coefficient is at its maximum, and consequently the predator isocline is at its lowest value on the *R*-axis (fig. 3.7*F*). At this point, the consumer has increased sufficiently in abundance to alter the overall fitness surface of the resource to favor lower trait values. The attack coefficient plummets as a result (fig. 3.7*C*), the consumer's abundance isocline then moves toward $+\infty$ on the *R*-axis, its abundance plummets, and the cycle begins again. All this merely causes a reversal in the direction of selection on the resource's trait, and not shifts between alternative adaptive peaks.

COEVOLUTION IN A SIMPLE ECOLOGICAL SYSTEM

Trait cycles show strikingly how the balance among selection gradients on underlying fitness components determine the directionality of trait change in both species, the dynamic nature of fitness and natural selection, and the coupling of abundance dynamics and coevolution for the two species. However, in much of parameter space, stable equilibria for the entire system result. The same types of dynamics occur as the system proceeds to a stable equilibrium, and the same balances are struck at these equilibria.

The outcome of coevolution between these two species depends on the ecological context in which their interaction takes place and on the underlying performance relationships between the traits and the various fitness components. For example, these two species may interact in various locations across the landscape (i.e., in different communities) that differ in many ways. One location may have high nutrient concentrations and good water availability in the soil, whereas another location may have nutrient-poor soils and low water availability. A plant species in these different areas would have a high intrinsic birth rate (c_0) in the community in the first location, but a low intrinsic birth rate in the second. The locations may also differ in conditions (e.g., temperature) that cause different levels of stress for the consumer or differ in the availability of other essential resources (e.g., water) that the consumer needs, and these differences may cause differences in the consumer's minimum intrinsic death rate (f_0) among locations. The maximum value of the attack coefficient (a_0) may also differ among communities because of environmental differences that cause prey to be more easily recognized or captured. For example, differences in turbidity would influence the ability of aquatic predators to see their prey, and different lakes may thus have different maximum possible values of attack coefficient. Locations may differ in structural complexity, and this also affects the ability of predators to capture prey. Alternatively, the maximum attack coefficient may take on different values because of other traits of the consumers and resources not being modeled here (e.g., visual acuity of the consumer); these also influence the likelihood of a prey being captured. These basic parameters reflect the abiotic features of the environment in which this species interaction occurs and other properties of the species' phenotypes not being modeled.

In this section, I explore how differences in these parameters, which will reflect differences in the ecological background of the community and other intrinsic properties of the species, affect the outcome of coevolution for these two species. I primarily present results for bidirectional-dependent traits underlying the attack coefficient, since parameter effects are generally the same across the various types of traits. However, I point out where discrepancies arise with other trait types. This is also not meant to be an exhaustive analysis of parameter space, but rather highlights the major trends.

First, consider the outcome of coevolution in communities that differ in productivity to cause differences in the resource's maximum intrinsic birth rate (c_0); see figure 3.8*A*–*B*. In a community where the c_0 is very low (e.g., <2.8 for the parameters considered in figure 3.8*A*–*B*), the resource is not abundant enough to support a consumer population, regardless of whether the consumer can evolve or not. In other words, the consumer is incapable of evolving to satisfy its invasibility criterion (i.e., equation (2.3)). As a result, the resource evolves to its intrinsic birth optimum (i.e., $\tilde{z}_R^c = 12.0$ in fig. 3.8*A*–*B*), and its abundance is $R^* = c(\tilde{z}_R^c)/d$.

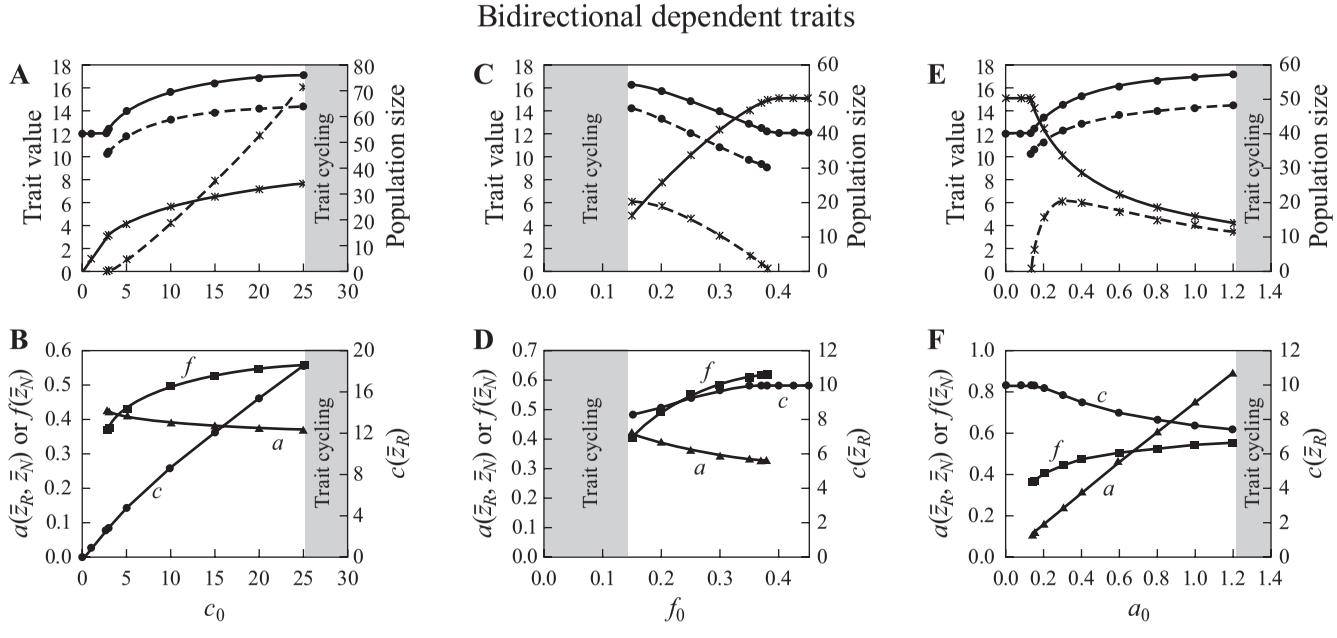

FIGURE 3.8. Effects of different values of (*A–B*) the resource's maximum intrinsic birth rate (c_0), (*C–D*) the consumer's minimum intrinsic death rate (f_0), and (*E–F*) the maximum attack coefficient (a_0) on the dynamics of coevolution between a resource and consumer with bidirectional-dependent traits defining the attack coefficients. Symbols identify equilibrium values for specific parameter combinations. The *top row* of panels shows the trait values (*filled circles*) and population sizes (×) for the resource (*solid lines*) and consumer (*dashed lines*). The *bottom row* of panels shows the realized values of the attack coefficient (*a*, *triangles*), resource intrinsic birth rate (*c*, *circles*) and consumer intrinsic death rate (*f*, *squares*). Parameter areas where trait cycling and population cycling occur are identified. Other parameters used in all these simulations are $c_0 = 10.0$, $d = 0.2$, $a_0 = 0.5$, $b = 0.1$, $h = 0.1$, $f_0 = 0.2$, $g = 0.0$, $\beta = 5.0$, $\gamma = 0.01$, $\theta = 0.01$, $\tilde{z}_R^c = 12.0$, $\tilde{z}_N^f = 1.0$, and $V_{z_R} = V_{z_N} = 0.2$. (Panels *A*, *C*, and *E* are redrawn from figure 3 of McPeek 2017, with permission).

In communities in which the resource has a maximum intrinsic birth rate above this critical value (e.g., >2.8 for the parameters considered in fig. 3.8*A–B*), the consumer can evolve to satisfy its invasibility criterion and thus support a local population. In this parameter range, in communities with higher values of c_0, the resource evolves to a trait value farther from its intrinsic birth optimum, and the consumer follows and then equilibrates at a trait value farther from its intrinsic death optimum (fig. 3.8*A–B*).

This latter result is caused by the ecological feedbacks between these two species. Larger values of c_0 caused the consumer to equilibrate at a higher abundance (chapter 2), which in turn causes a steeper selection gradient on the resource's death fitness component. As a result, the resource strikes the balance between the selection gradients of its two fitness components farther from its intrinsic birth optimum ($\tilde{z}_R^c$). In addition, the higher resource productivity increases the consumer's realized birth rate, which allows it to support a population at a higher realized death rate (fig. 3.8*B*); this in turn permits it to strike the balance between the selection gradients of its fitness components farther from its intrinsic death optimum ($\tilde{z}_N^f$). Thus, the productivity of the environment affecting the resource only indirectly influences which trait value is favored for it by determining the consumer's abundance. Yet again, we cannot understand the outcome of coevolution without understanding the drivers of species abundances.

A similar line of explanation holds when comparing communities that develop in locations with different environmental conditions that cause differences in the consumer's minimum intrinsic death rate (f_0) (fig. 3.8*C–D*). If f_0 is too high in a particular location, again the consumer is incapable of evolving to support a population (e.g., $f_0 > 0.39$ for the parameters considered in fig. 3.8*C–D*). Below this point, the consumer will evolve farther from its intrinsic death optimum in communities in which it has a lower f_0 value, which also forces the resource to evolve farther from its intrinsic birth optimum. A lower value of f_0 results in a lower intrinsic death rate for the consumer at a given trait value (fig. 3.8*D*), which results in a larger consumer abundance (fig 3.8*C*); this in turn causes a steeper selection gradient on the resource's death fitness component.

Likewise, the outcome of coevolution will differ between communities with environmental differences that would affect the maximum value of the attack coefficient (a_0) (fig. 3.8*E–F*). Here again, if the maximum attack coefficient is too low, the consumer will not be able to support a population, even if it can evolve (e.g., $a_0 < 0.135$ for the parameters considered in fig. 3.8*E–F*). Because a higher value of a_0 will directly create steeper selection gradients on both the resource's death fitness component and the consumer's birth fitness component, both species will evolve to trait values that are farther from their respective intrinsic optimal phenotypes in communities where a_0 is larger (fig. 3.8*E*).

These results suggest a general set of predictions that can be easily tested. For example, they predict that selection gradients on fitness components will be steeper in species up and down the food web in communities (1) with higher basal productivity (results for larger c_0), (2) with more benign conditions for the consumer (lower f_0), and (3) where environmental conditions permit the consumer to catch resources at higher maximum rates (higher a_0). Moreover, if one interprets the distance from the intrinsic birth optimum as a measure of the elaboration of an antipredator defense (e.g., swimming faster, producing more of a noxious chemical, lengthening spines, making exceedingly large or small seeds), prey should also evolve more elaborate defenses in communities with these same environmental conditions (i.e., higher basal productivity, more benign conditions for consumers, and higher maximal capture rates). Also, changes in species abundances across these environmental conditions match what one would expect purely based on ecological considerations—namely, abundances of both species should increase with productivity, the resource should increase with increasing death rate of the consumer, and the resource should decline and the abundance of the consumer should first increase and then decrease with an increasing attack coefficient (cf. fig. 3.8 with results in chapter 2). Therefore, species coevolution should reinforce ecological patterns of community structure along environmental gradients.

The steepness of the underlying selection gradient on the various fitness components (i.e., the shapes of the relationships in fig. 3.1 controlled by γ, θ, β, α, or ε_R, and ε_N) may also differ among communities, or among different consumer-resource interaction pairs within a community. For example, in an environment in which the distance to safety (e.g., thick bushes for cover) is very short, a resource species many only need to run slightly faster than its consumer to effectively evade capture; but in an environment in which the distance to safety is far, the resource species may need to be substantially faster than the consumer to have the same chances of escaping capture. These environments would cause a difference in α for the unidirectional-dependent traits of escape and pursuit speed (fig. 3.1*D*), and this difference will influence how the consumer and resource coevolve, because the positions of evolutionary equilibria are set by the balance of selection gradients on different fitness components.

Because the relative strengths of the selection gradients acting on different fitness components determine the shape of the overall fitness surface against which the species evolve (Arnold and Wade 1984b, McPeek 1996b), differences in the underlying selection gradients will also shape the outcome of coevolution. For example, compare the result of coevolution in communities where the coefficient scaling the change in the attack coefficient with bidirectional-dependent traits (i.e., where a smaller β value makes the gradient steeper). If the realized attack coefficient changes very slowly with a change in the difference in species' trait

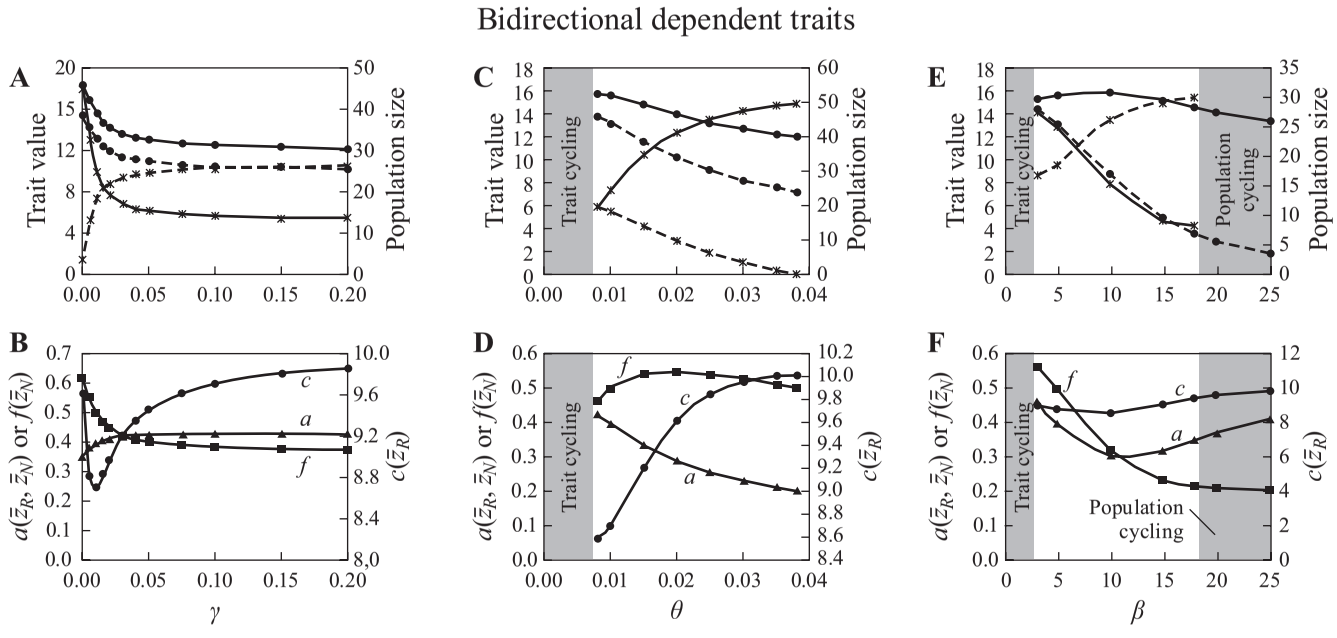

FIGURE 3.9. Effects of different values of (*A–B*) the underlying selection strength for the resource intrinsic birth rate and the minimum value (γ), (*C–D*) the underlying selection strength for the consumer intrinsic death rate (θ), and (*E–F*) the underlying selection strength for the attack coefficient (β) on the dynamics of coevolution between a resource and consumer with bidirectional-dependent traits defining the attack coefficients. Symbols identify equilibrium values for specific parameter combinations. Panels and symbols are as given in figure 3.8. Parameter areas where trait cycling occurs are identified. Parameters in these simulations are the same as those used for the results presented in figure 3.8. (Panels *A*, *C*, and *E* are redrawn from figure 3 of McPeek 2017, with permission).

values (i.e., large value of β), the consumer does not have to evolve far from its intrinsic death optimum to capture substantial quantities of resources (fig. 3.9*E–F*). Making the intrinsic gradient on the attack coefficient steeper (i.e., smaller β) causes the consumer to be closer to the resource's trait value, which moves it farther from its intrinsic death optimum, and thus causes the consumer's abundance to decrease and the resource's abundance to increase. Interestingly, differences in β have little effect on the resource's trait value; the realized selection gradient on the resource's death fitness component changes little because the increase in the attack coefficient is offset by the decrease in the consumer's abundance.

Altering the intrinsic gradients on the resource's intrinsic birth rate (i.e., γ in equation (3.12)) or the consumer's intrinsic death rate (i.e., θ in equation (3.13)) also change the outcome of coevolution (fig. 3.9*A–D*). A steeper intrinsic gradient on the resource's intrinsic birth rate (increasing γ) forces the resource to evolve a trait value closer to its intrinsic birth optimum (fig. 3.9*A–B*), and the analogous result is true for the consumer (fig. 3.9*C–D*). For example, higher values of θ cause the consumer to evolve with have a trait value closer to $\tilde{z}_N^f$, which decreases the realized attack coefficient (fig. 3.9*C–D*). As a consequence of the decreased realized attack coefficient, the resource will evolve to have a trait value closer to $\tilde{z}_R^c$. If the consumer cannot support a population in the system at $\bar{z}_N = \tilde{z}_N^f$ (as for the parameters considered in fig. 3.9*C–D*), high values of θ (i.e., strong intrinsic selection gradient on the consumer's death fitness component) will prevent the consumer from existing in the system, even with adaptation. These considerations illustrate the critical importance of quantifying the strengths of selection gradients on various fitness components to understand the overall form and outcome of natural selection.

Finally, the distance between the intrinsic trait optima, $\tilde{z}_R^c$ and $\tilde{z}_N^f$, of the consumer and resource also strongly shapes the ecological system that will evolve, and the importance of the absolute distance between them depends on the underlying selection gradient of the attack coefficient. I show results for each trait type underlying the attack coefficients here because the effect of increasing $\tilde{z}_R^c$ relative to $\tilde{z}_N^f$ depends on the attack coefficient traits. The consequences of altering the distance between $\tilde{z}_N^f$ and $\tilde{z}_R^c$ illustrate the main difference between the three trait types. Since the consumer does not have to match the resource in phenotype in any particular way when independent traits underlie the attack coefficient, altering $\tilde{z}_R^c$ relative to $\tilde{z}_N^f$ has little effect on the abundances of the two species over much of this range; the prey is then the primary species to evolve, regardless of the selection strength (fig. 3.10*A–D*). In addition, if the resource's optimum is near the value where the realized attack coefficient would be very low, the consumer may not be able to support a population (fig. 3.10*A–D*).

In contrast, increasing the distance between $\tilde{z}_R^c$ and $\tilde{z}_N^f$ for unidirectional and bidirectional-dependent traits can eventually drive the consumer extinct as it

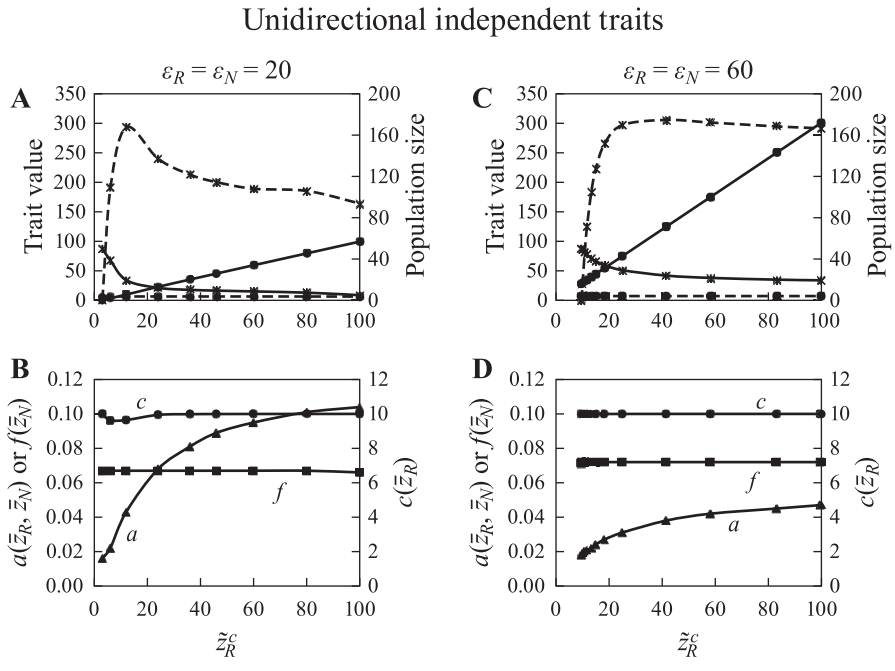

FIGURE 3.10. Effects of different values of the resource's intrinsic birth optimum $\tilde{z}_R^c$ for various levels of the underlying selection strengths for the attack coefficients when (*A–D*) unidirectional-independent traits, (*E–J*) unidirectional-dependent traits, and (*K–P*) bidirectional-dependent traits on the dynamics of coevolution between a resource and consumer. Panels and symbols are as given in figure 3.8. The underlying selection strength parameters used in simulations are given above the column of panels. Other parameters used in simulations are as follows: unidirectional-independent traits (panels *A–D*) $c_0 = 10.0$, $d = 0.2$, $a_0 = 0.5$, $b = 0.1$, $h = 0.3$, $f_0 = 0.05$, $g = 0.0$, $\gamma = 0.01$, $\theta = 0.01$, $\tilde{z}_N^f = 1.0$, $V_{z_R} = V_{z_N} = 0.2$; unidirectional-dependent traits (panels *E–J*) $c_0 = 10.0$, $d = 0.2$, $a_0 = 0.5$, $b = 0.1$, $h = 0.3$, $f_0 = 0.05$, $g = 0.0$, $\gamma = 0.01$, $\theta = 0.01$, $\tilde{z}_N^f = 1.0$, $V_{z_R} = V_{z_N} = 0.2$; and bidirectional-dependent traits (panels *K–P*) $c_0 = 10.0$, $d = 0.2$, $a_0 = 0.5$, $b = 0.1$, $h = 0.1$, $f_0 = 0.2$, $g = 0.0$, $\gamma = 0.01$, $\theta = 0.01$, $\tilde{z}_R^c = 12.0$, $\tilde{z}_N^f = 1.0$, $V_{z_R} = V_{z_N} = 0.2$.

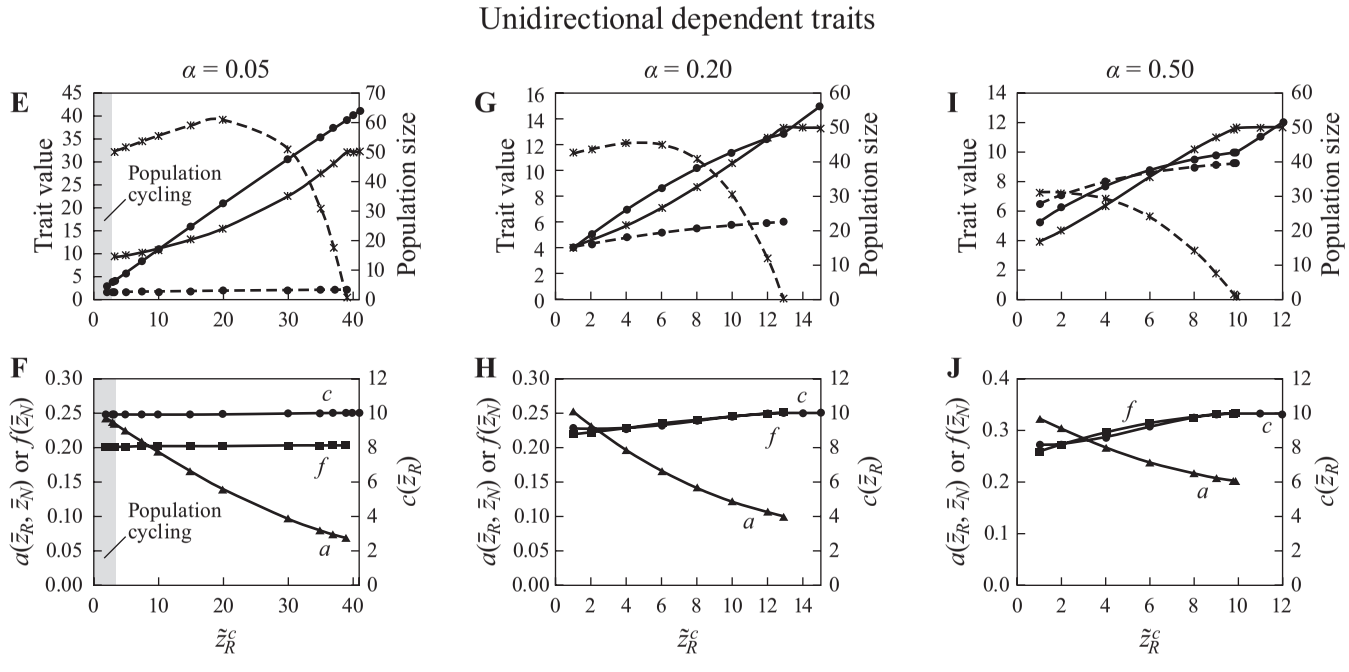

coevolves away from its intrinsic death rate optimum to maintain an adequate capture rate of the resource (fig. 3.10*E–P*). Stronger selection on the attack coefficient (i.e., larger values of α or lower values of β) also causes the consumer to evolve to extinction at lower values of $\tilde{z}_R^c$ relative to $\tilde{z}_N^f$ (fig. 3.10*E–P*).

ADD A TROPHIC LEVEL

Now consider how this simple consumer-resource system evolves when a predator that feeds on the consumer (i.e., a third trophic level), and potentially the resource as well (i.e., an intraguild predator), is added to the system. The predator feeds on the consumer, and possibly the resource, both with a saturating functional response (i.e., intraguild predation/omnivory) and experiences its own density-dependent death rate. Adding this predator to the system elaborates the dynamical abundance and trait system to the following general form:

$$
\begin{aligned}
\frac{dP}{dt} &= P\ln(\bar{W}_P) = P\left(\frac{wv(\bar{z}_R,\bar{z}_p)R + nm(\bar{z}_R,\bar{z}_p)N}{1+v(\bar{z}_R,\bar{z}_p)uR+m(\bar{z}_R,\bar{z}_p)lN} - x(\bar{z}_P) - yP\right)\\
\frac{dN}{dt} &= N\ln(\bar{W}_N) = N\left(\frac{ba(\bar{z}_R,\bar{z}_N)R}{1+a(\bar{z}_R,\bar{z}_N)hR} - \frac{m(\bar{z}_R,\bar{z}_p)P}{1+v(\bar{z}_R,\bar{z}_p)uR+m(\bar{z}_R,\bar{z}_P)lN} - f(\bar{z}_N) - gN\right)\\
\frac{dR}{dt} &= R\ln(\bar{W}_R) = R\left(c(\bar{z}_R) - dR - \frac{a(\bar{z}_R,\bar{z}_N)N}{1+a(\bar{z}_R,\bar{z}_N)hR} - \frac{wv(\bar{z}_R,\bar{z}_p)P}{1+v(\bar{z}_R,\bar{z}_p)uR+m(\bar{z}_R,\bar{z}_P)lN}\right)\\
\frac{d\bar{z}_P}{dt} &= V_{z_P}\left(\left.\frac{wR\frac{\partial v(\bar{z}_R,z_p)}{\partial z_P} + nN\frac{\partial m(\bar{z}_N,z_P)}{\partial z_P} + RN(nu-wl)\left(v(\bar{z}_R,z_p)\frac{\partial m(\bar{z}_N,z_P)}{\partial z_P} - m(\bar{z}_N,z_P)\frac{\partial v(\bar{z}_R,z_p)}{\partial z_P}\right)}{(1+v(\bar{z}_R,z_p)uR+m(\bar{z}_R,z_p)lN)^2}\right|_{z_P=\bar{z}_P} - \left.\frac{\partial x(z_P)}{\partial z_P}\right|_{z_P=\bar{z}_P}\right).\\
\frac{d\bar{z}_N}{dt} &= V_{z_N}\left(\left.\frac{bR\frac{\partial a(\bar{z}_R,z_N)}{\partial z_N}}{(1+a(\bar{z}_R,z_N)hR)^2}\right|_{z_N=\bar{z}_N} - \left.\frac{P\frac{\partial m(z_N,\bar{z}_P)}{\partial z_N}}{1+v(\bar{z}_R,\bar{z}_p)uR+m(\bar{z}_R,\bar{z}_p)lN}\right|_{z_N=\bar{z}_N} - \left.\frac{\partial f(z_N)}{\partial z_N}\right|_{z_N=\bar{z}_N}\right)\\
\frac{d\bar{z}_R}{dt} &= V_{z_R}\left(\left.\frac{\partial c(z_R)}{\partial z_R}\right|_{z_R=\bar{z}_R} - \left.\frac{N\frac{\partial a(z_R,\bar{z}_N)}{\partial z_R}}{(1+a(\bar{z}_R,\bar{z}_N)hR)}\right|_{z_R=\bar{z}_R} - \left.\frac{P\frac{\partial v(z_R,\bar{z}_P)}{\partial z_R}}{1+v(\bar{z}_R,\bar{z}_p)uR+m(\bar{z}_R,\bar{z}_P)lN}\right|_{z_N=\bar{z}_N}\right)
\end{aligned}
\tag{3.20}
$$

In the added functional responses, $m(\bar{z}_N,\bar{z}_P)$ is the attack coefficient, n is the conversion efficiency, and l is the handling time for the predator feeding on the consumer; $v(\bar{z}_R,\bar{z}_P)$ is the attack coefficient, w is the conversion efficiency, and u is the handling time for the predator feeding on the resource.

The predator also has an intrinsic death rate given by $x(\bar{z}_P)$ and a density-dependent increase in death rate defined by y. The functions describing the

relationships between trait and parameter values follow the same form as those for the consumer. The functions defining the two attack coefficients of the predator for the different trait types are given in box 3.1. The intrinsic death rate is given by

$$x(z_p) = x_0\left(1 + \delta(z_p - \tilde{z}_P^x)^2\right), \tag{3.21}$$

where $\tilde{z}_P^x$ is the trait value that minimizes the predator's intrinsic death rate, x_0 is the minimum intrinsic death rate at this optimum when $z_p = \tilde{z}_P^x$, and δ mediates the underlying selection gradient on z_P due to the death fitness component.

First, consider the evolution of this system in the absence of intraguild predation (i.e., $v(\bar{z}_R, \bar{z}_P) = 0$). The first general feature to emerge when a third trophic level is added to create a food chain is that the basal resource generally evolves trait values that are closer to its own intrinsic birth optimum as compared to when the predator is not feeding on the consumer (fig. 3.11). If the predator can invade, adapt, and ultimately support a population, it reduces the consumer's abundance and alters the trait value favored in the consumer, which in turn changes the attack coefficient of the consumer feeding on the resource. Thus, the presence of the predator alters both the ecological (i.e., consumer's abundance) and evolutionary (i.e., consumer's trait value) conditions experienced by the resource. When the attack coefficient between the predators and their prey are determined by unidirectional-dependent (fig. 3.11*E–H*) or bidirectional-dependent traits (fig. 3.11*I–L*), the realized attack coefficient between the consumer and resource increases in the presence of the predator because of changes in both the consumer's and resource's phenotypes. Despite the increase in the attack coefficient on the resource, the reduction in the consumer's abundance reduces the selection gradient sufficiently on the resource's death fitness component to favor a trait value closer to $\tilde{z}_R^c$ in the presence of the predator.

If the attack coefficients are determined by unidirectional-independent traits (fig. 3.11*A–D*), the consumer evolves a lower trait value that lowers the attack coefficient on itself from the predator, which concomitantly reduces its own attack coefficient on the resource. Here, the resource evolves to have a phenotype closer to its intrinsic birth optimum, because of both an evolutionary reduction in the attack coefficient on it and an ecological reduction in the consumer's abundance. Thus, the types of traits involved in the species interactions determine how the ecological structure and interaction strengths among species change as new species are added to a community.

Comparing communities with different maximum attack coefficients of the predator on the consumer, m_0 has little effect on the trait value that is favored in the predator (fig.3.11*C*, *G*, and *K*). However, communities with higher values of m_0 have lower abundances of both the predator and the consumer, which causes the resource to evolve a trait value closer to its intrinsic birth optimum. Different

Box 3.1. Functions for three different trait types defining the predator attack coefficients

When a top predator is added to a simple system containing a basal resource and an intermediate consumer, two additional functional responses must be defined. These are given in equations (3.20). Thus, an attack coefficient for the predator feeding on each must also be defined that incorporates the effects of the phenotypic traits of the interacting species to determining the realized value of each in the model. Thus, $m(z_N, z_P)$ is the attack coefficient of the predator feeding on the consumer, and $v(z_R, z_P)$ is the attack coefficient of the predator feeding on the resource.

When unidirectional-independent traits define each, the functional forms are

$$m(z_N, z_P) = \frac{m_0 z_N z_P}{(\eta_N + z_N)(\eta_P + z_P)} \;\; \& \;\; v(z_R, z_P) = \frac{v_0 z_R z_P}{(\kappa_R + z_N)(\kappa_P + z_P)}.$$

As with the analogous equation (i.e., equation [3.14]) for the consumer feeding on the resource, m_0 and v_0 are the asymptotic maxima for each, and η_x and κ_x are scaling parameters that define the underlying selection strength for the respective species traits.

When unidirectional-dependent traits define these attack coefficients, the functional forms are

$$m(z_N, z_P) = \frac{m_0}{1 + e^{-\rho\Omega}} \;\; \& \;\; v(z_R, z_P) = \frac{v_0}{1 + e^{-\tau\Sigma}},$$

where $\Omega = z_P - z_N$ and $\Sigma = z_P - z_R$, and ρ and τ are scaling parameters that define the underlying selection strengths on the respective attack coefficients in this case.

When bidirectional-dependent traits define these attack coefficients, the functional forms are

$$m(z_N, z_P) = m_0 e^{-\left(\frac{\Omega}{\phi}\right)^2} \;\; \& \;\; v(z_R, z_P) = v_0 e^{-\left(\frac{\Sigma}{\psi}\right)^2},$$

where ϕ and ψ are scaling parameters that define the underlying selection strengths on the respective attack coefficients in this case.

values of the underlying selection strength on $m(\bar{z}_N, \bar{z}_P)$ cause different trait values that evolve in the predator, giving a higher realized value of $m(\bar{z}_N, \bar{z}_P)$ with stronger underlying selection (fig. 3.11*D*, *H*, and *L*).

Communities with higher productivity of the basal resource (i.e., larger values of c_0) have higher abundances of all three species regardless of the trait

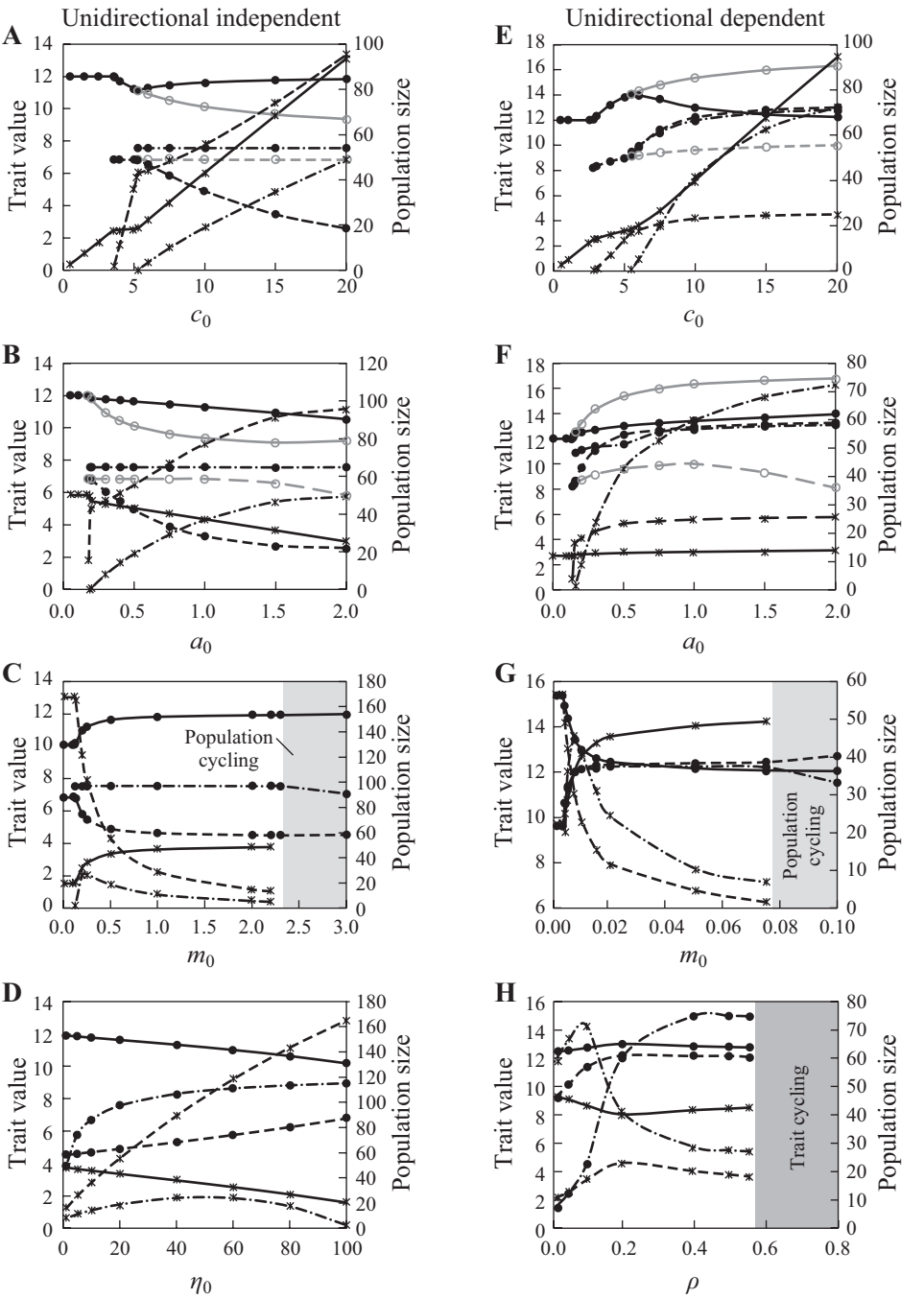

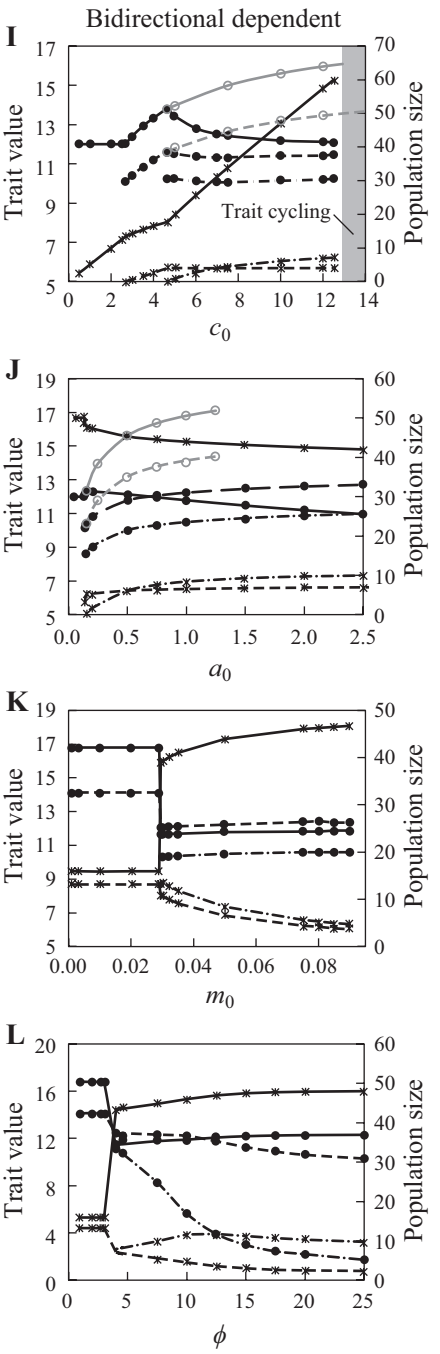

FIGURE 3.11. Effects of different values of the maximum intrinsic birth rate of the resource (c_0), the maximum attack coefficient of the consumer on the resource (a_0), the maximum attack coefficient of the predator on the consumer (m_0), and the various underlying selection strengths (η_P, ρ, ϕ) on the attack coefficient of the predator on the consumer; these are for the various trait types on the dynamics of coevolution in a three trophic level food chain with one species at each trophic level. Each panel shows the trait values (*filled circles*) and population sizes (×) for the resource (*solid lines*), consumer (*dashed lines*), and predator (*dot-dashed lines*). Results from simulations in which the predator is absent are shown in *gray*, so that the effects of adding the top predator can be compared. The *left column* shows results for simulations where all attack coefficients are defined by unidirectional-independent traits, the *middle column* for unidirectional-dependent traits, and the *right column* for bidirectional-dependent traits. Parameter areas where trait cycling and population cycling occur are identified. Parameters other than the gradient parameter used in simulations are as follows: unidirectional-independent traits (panels *A–D*) $c_0 = 10.0$, $d = 0.2$, $a_0 = 0.5$, $b = 0.1$, $h = 0.3$, $m_0 = 0.05$, $n = 0.1$, $l = 0.3$, $f_0 = 0.05$, $g = 0.0$, $x = 0.01$, $y = 0.0$, $\varepsilon_R = 20.0$, $\varepsilon_N = 20.0$, $\gamma = 0.01$, $\eta_N = 20.0$, $\eta_P = 20.0$, $\theta = 0.01$, $\delta = 0.01$, $\tilde{z}_R^c = 20.0$, $\tilde{z}_N^f = 1.0$, $\tilde{z}_P^x = 1.0$, $V_{z_R} = V_{z_N} = V_{z_P} = 0.2$; unidirectional-dependent traits (panels *E–H*) $c_0 = 10.0$, $d = 0.2$, $a_0 = 0.5$, $b = 0.1$, $h = 0.2$, $m_0 = 0.01$, $n = 0.1$, $l = 0.2$, $f_0 = 0.2$, $g = 0.0$, $x = 0.01$, $y = 0.0$, $\alpha = 0.1$, $\rho = 0.1$, $\gamma = 0.01$, $\theta = 0.01$, $\delta = 0.01$, $\tilde{z}_R^c = 12.0$, $\tilde{z}_N^f = 1.0$, $\tilde{z}_P^x = 1.0$, $V_{z_R} = V_{z_N} = V_{z_P} = 0.2$; and bidirectional-dependent traits (panels *I–L*) $c_0 = 10.0$, $d = 0.2$, $a_0 = 1.0$, $b = 0.1$, $h = 0.1$, $m_0 = 0.05$, $n = 0.1$, $l = 0.1$, $f_0 = 0.2$, $g = 0.0$, $x = 0.01$, $y = 0.0$, $\beta = 5.0$, $\phi = 5.0$, $\gamma = 0.01$, $\theta = 0.01$, $\delta = 0.02$, $\tilde{z}_R^c = 12.0$, $\tilde{z}_N^f = 1.0$, $\tilde{z}_P^x = 1.0$, $V_{z_R} = V_{z_N} = V_{z_P} = 0.2$.

types underlying the attack coefficients (fig. 3.11*A*, *E*, and I). The evolutionary responses of the three species when c_0 is greater are more heterogeneous. Higher values of c_0 cause the resource to evolve closer to its intrinsic birth optimum for all trait types underlying the attack coefficients, but the evolutionary responses in the consumer and predator depend on the trait types. The phenotype of the predator responds to different levels of productivity of the resource substantially only when unidirectional-dependent traits determined the attack coefficients (fig. 3.11*E*), whereas with higher values of c_0, the consumer evolves closer to its intrinsic death optimum with unidirectional-independent traits (fig. 3.11*A*) and away from its intrinsic death optimum with unidirectional-dependent traits (fig. 3.11*E*).

The evolutionary responses of species at the three trophic levels when the top predator is also an intraguild predator differs depending on the trait types defining the attack coefficients (fig. 3.12). With both independent- and dependent-unidirectional traits defining the attack coefficients, a higher maximum value of the attack coefficient for the predator feeding on the resource (v_0) causes smooth transitions in trait values for all species across communities. In communities with higher values of v_0, the resource evolves to a trait value closer to its intrinsic birth rate optimum, the consumer evolves farther from its intrinsic death rate optimum, and the predator evolves closer to its intrinsic birth optimum (fig. *3.12A–B*). With high values of v_0 at which the consumer cannot persist, the system returns to two trophic levels.

In contrast, when bidirectional-dependent traits define the attack coefficients, higher values of v_0 result in more graded transitions (fig. 3.12*C*). Over a range of low values of v_0 (0.0001–0.0015 in fig. 3.12*C*), changing its value has little effect on the traits that evolve in the three species or their abundances, with the predator having a trait value between the resource and consumer. Above this range, the predator evolves to feed more heavily on the resource by shifting its trait value below that of the resource and thus closer to its intrinsic death rate optimum. Here again, the outcome of coevolution by natural selection critically depends on the structure of the community and on the trait types defining the species interactions.

IMPLICATIONS FOR MEASURING SELECTION IN THE WILD

This theoretical exploration of the ecological dynamics of natural selection provides important guidance into what measures of natural and sexual selection in wild populations quantify. First, few if any studies of natural selection in a wild population actually measure overall fitness. The studies that come the closest are those that follow marked populations of large mammals over multiple generations (e.g., Ozgul et al. 2009). However, most studies take a snapshot of selection within

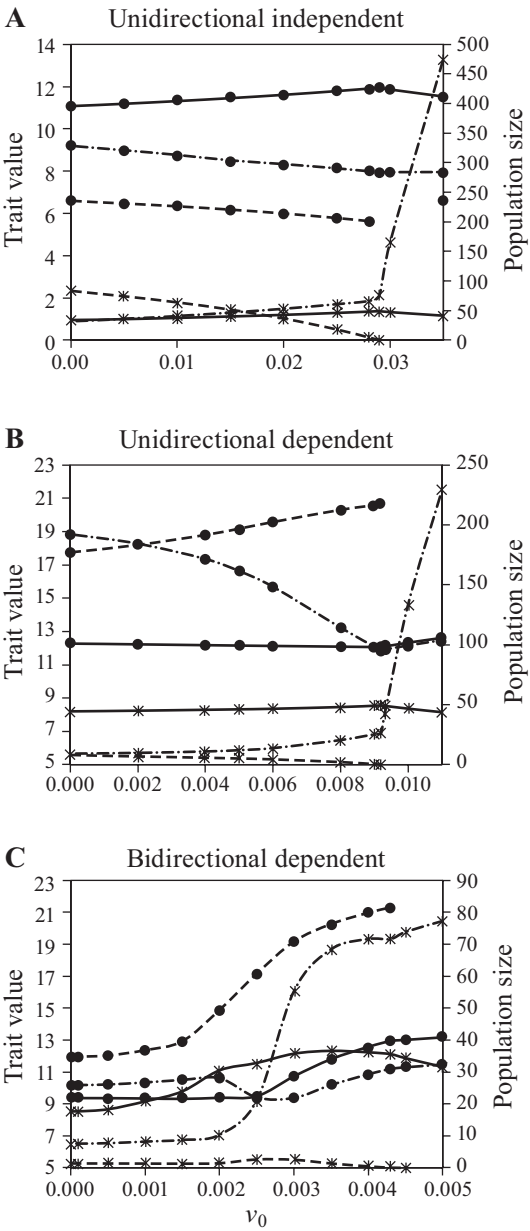

FIGURE 3.12. Effects of different values of the predator's maximum attack coefficient on the resource (v_0) (i.e., the strength of intraguild predation) for the various trait types on the dynamics of coevolution in a three-trophic-level food chain with one species at each trophic level. (*A*, unidirectional-independent traits; *B*, unidirectional-dependent traits; and *C*, bidirectional-dependent traits.) Symbols are as specified in figure 3.11. Parameters other than the gradient parameter used in simulations are as follows: (*A*) unidirectional-independent traits $c_0 = 10.0$, $d = 0.2$, $a_0 = 0.5$, $b = 0.1$, $h = 0.1$, $m_0 = 0.1$, $n = 0.1$, $l = 0.1$, $w = 0.1$, $u = 0.1$, $f_0 = 0.05$, $g = 0.0$, $x = 0.01$, $y = 0.0$, $\varepsilon_R = 20.0$, $\varepsilon_N = 20.0$, $\eta_N = 20.0$, $\eta_P = 20.0$, $\kappa_R = 20.0$, $\gamma = 0.01$, $\theta = 0.01$, $\delta = 0.01$, $\tilde{z}_R^c = 20.0$, $\tilde{z}_N^f = 1.0$, $\tilde{z}_P^x = 1.0$, $V_{z_R} = V_{z_N} = V_{z_P} = 0.2$; (*B*) unidirectional-dependent traits $c_0 = 10.0$, $d = 0.2$, $a_0 = 0.5$, $b = 0.2$, $h = 0.1$, $m_0 = 0.1$, $n = 0.1$, $l = 0.1$, $w = 0.1$, $u = 0.1$, $f_0 = 0.2$, $g = 0.0$, $x = 0.01$, $y = 0.0$, $\alpha = 0.2$, $\rho = 0.2$, $\tau = 0.2$, $\gamma = 0.01$, $\theta = 0.01$, $\delta = 0.01$, $\tilde{z}_R^c = 12.0$, $\tilde{z}_N^f = 1.0$, $\tilde{z}_P^x = 1.0$, $V_{z_R} = V_{z_N} = V_{z_P} = 0.2$; and (*C*) bidirectional-dependent traits $c_0 = 1.0$, $d = 0.\ 02$, $a_0 = 0.75$, $b = 0.1$, $h = 0.05$, $m_0 = 0.1$, $n = 0.1$, $l = 0.05$, $w = 0.1$, $u = 0.05$, $f_0 = 0.005$, $g = 0.0$, $x = 0.005$, $y = 0.0$, $\beta = 5.0$, $\phi = 5.0$, $\psi = 5.0$, $\gamma = 0.02$, $\theta = 0.02$, $\delta = 0.02$, $\tilde{z}_R^c = 12.0$, $\tilde{z}_N^f = 1.0$, $\tilde{z}_P^x = 1.0$, $V_{z_R} = V_{z_N} = V_{z_P} = 0.2$.

one generation, and typically only on a subset of the entire life cycle of the organism being studied. Most also consider only one fitness component. For example, in their comprehensive analysis of selection measures in the wild, Kingsolver et al. (2001) divided the studies they found into three categories based on what measure of fitness was being considered: survival, mating success, or fecundity. Not surprisingly, they found that linear (i.e., directional) selection was common, but quadratic selection was not (see also Hendry and Kinnison 1999, Hoekstra et al. 2001, Rieseberg et al. 2002, Kingsolver and Diamond 2011, Kingsolver et al. 2012). Quadratic selection is a measure of the curvature of the fitness surface experienced by the population and is a necessary but not sufficient condition for the identification of stabilizing or disruptive selection.

The theoretical investigations presented here suggest that measures of selection on fitness components should most frequently identify directional selection as important, since the evolution of a species typically reaches an equilibrium at which the selection gradients of different fitness components balance (e.g., fig. 3.3*C*). Thus, directional selection being found more frequently is not surprising, especially since stabilizing and disruptive selection should also be harder to identify (Haller and Hendry 2014), and most studies of phenotypic selection in the wild measure fitness components and not lifetime overall fitness. Moreover, even if multiple fitness components are influenced by bidirectional traits, the balance required will typically mean that few if any fitness components will be at their optimal trait values.

However, these analyses also found little evidence for trade-offs among selection pressures, which should be the signature of such balancing selection gradients (i.e., the selection gradients summing to zero in equation (3.7)); see Kingsolver et al. 2001, Kingsolver and Diamond 2011, Kingsolver et al. 2012). For example, in one compilation of studies, the magnitude and direction of selection was found to balance in only 2% of the cases in which multiple fitness components were measured in association with one trait (Kingsolver and Diamond 2011). These authors offer a number of plausible reasons for why evidence of such expected fitness trade-offs is sparse among the data, including that the various fitness components or traits involved in the trade-off were not all included in the analyses, spatial environmental variation influences multiple fitness components simultaneously (e.g., Rausher 1992, Stinchecombe et al. 2002), selection varied temporally in direction, and indirect selection occurred on correlated traits.

The most likely culprit for the lack of evidence for fitness trade-offs is that optimizing selection rarely results from the simple balance of only two opposing selection gradients operating on one trait in real organisms. The models considered in this chapter only included two overall fitness components (birth and death rates) acting on one trait. However, even for this simple scenario, many more

than two selection gradients may act on a single trait—particularly when a demographic rate is influenced by multiple selection gradients, as when the species interacts with more than one species. We will see much more of this in chapter 5, but even in the models considered in this chapter, the resource evolves to balance three fitness components when a consumer and an intraguild predator are present (equation (3.20)). One would conclude that the resource's fitness components balance only when all three are measured simultaneously. To properly see the balancing in this case, the resource's survival would have to also be separated into the components due to predation by the intraguild prey and intraguild predator. If interactions with many more species are also considered, as well as multiple traits influencing various fitness components, and the fact that one must measure fitness components over the entire life cycle of an organism, then the task for actually identifying where the trade-offs lie becomes daunting, if not impossible.

Given the ubiquity of directional selection that is apparent in these summary analyses, one must ask also why rapid changes in the phenotypes of species are not occurring (Merilä et al. 2001). This is a particularly troubling question given the consistency in the direction of selection over multiple generations measured in many species (Siepielski et al. 2009, Kingsolver and Diamond 2011, Siepielski et al. 2011a, Siepielski et al. 2013). Many plausible explanations exist for how consistent selection gradients that a population experiences generation after generation may still result in little if any phenotypic change over time, particularly since heritabilities of many traits under selection seems to be adequate to permit responses (Mousseau and Roff 1987). These include strong antagonistic genetic correlations that prevent response to selection, unmeasured countervailing selection pressures, and greater environmental phenotypic variation in natural populations (see Merilä et al. 2001 for an excellent discussion of these).

The theoretical analyses presented here suggest an additional explanation that is actually embodied in all of these, but one that will be difficult to document for the reasons given in the previous paragraph. This explanation is that many species are at evolutionary equilibria. The direction of selection is consistent across years and generations in many species, whereas the magnitudes of the selection gradients do fluctuate (Siepielski et al. 2009, Kingsolver and Diamond 2011, Siepielski et al. 2011a). These conditions would be expected for species at or near the point where the selection gradients they experience are relatively balanced, but short-term fluctuations in the abundances of interacting species cause the magnitudes to vary. This short-term variability is probably caused by short-term fluctuations in abiotic conditions that affect the magnitudes of species' intrinsic birth and death rates. Large and changing types of selection should be expected most when species are first adapting to a new selection regime (e.g., figs. 3.2 and 3.3), as when they are introduced into a new environment (Hendry and Kinnison 1999).

THE BALANCE THAT IS STRUCK

The outcome of coevolutionary interactions among species is determined by the balances that are struck among both the fitness components and selection gradients experienced by each species. Also, the outcomes of these coevolutionary interactions influence both what evolves in each species and the abundance dynamics that results in the community.

If the community reaches a stable equilibrium point in both abundances and traits, the balancing fitness components in each species are what generates stability of the abundances. At equilibrium, the overall realized birth and death rates sum to zero for each species, with these abundances being defined by the position where their abundance isoclines intersect (chapter 2). I hope it was clear that everything considered in chapter 2 applies when we consider the community's evolutionary aspects. The only difference with evolutionary dynamics is that the abundance isoclines for the species change shape and position as their traits change in evolutionary response to one another.

The evolutionary balance requires that the selection gradients for each species also sum to zero. The selection gradients are defined by the underlying relationships of fitness components with the traits experiencing selection; and the relative magnitudes of these selection gradients for the various fitness components will define the outcome of that selective process. In other words, if the selection gradient associated with one fitness component is disproportionately strong relative to all others, the overall fitness surface's shape will be defined primarily by this selection gradient, and the species will consequently evolve mostly in response to this selection gradient (McPeek 1996a). For example, when the underlying selection strength on the resource's intrinsic birth rate is high (i.e., large γ) relative to the other fitness components, the resource evolves a trait value very close to its intrinsic birth optimum (fig. 3.9*A*). However, when the underlying selection gradient on the attack coefficient is relatively high (i.e., small β), the resource evolves farther from its intrinsic birth optimum if that will decrease predation, and the consumer will evolve farther from its intrinsic death optimum (fig. 3.9*E*).

The best theoretical illustrations of the importance of this balance are when trait cycling occurs. Trait cycling takes place when the balance among selection gradients continually shift back and forth. In the models studied here, prey will periodically evolve to become more vulnerable to their predators when the selection gradients on other fitness components are stronger. This cycling only occurs in areas of parameter space where the underlying selection strengths are relatively equal (fig. 3.6).

The magnitudes of the fitness components also influence the balance struck among the various selection gradients impinging on each species. For example, increasing its maximum intrinsic birth rate permits the resource to evolve farther from its intrinsic birth optimum; similarly decreasing the consumer's minimum intrinsic death rate permits it to evolve farther from its intrinsic death optimum. Moreover, because many of the fitness components are influenced by the abundances of themselves or other species, alterations of these parameters in one species can shift these balances merely by changing features of the system that alter species abundances (e.g., the strength of density dependence). In other words, one cannot determine what trait value will be favored in one species without knowing the abundances of all species with which it interacts in the community.

All these considerations imply that a much richer ecological and evolutionary set of information is needed if we are to actually understand various patterns of natural selection in the wild. Moreover, this richer set of considerations makes the study of natural selection a *predictive endeavor*. Given the last few paragraphs, one would predict that a resource species in a productive environment would adapt primarily by elaborating defenses to thwart its enemies (e.g., predators, diseases), whereas the same resource species in an unproductive environment would adapt primarily by adapting to maximize its birth rate at the expense of defenses against enemies (fig. 3.8). However, in the productive environment one would measure a strong selection gradient for its birth rate (because the species is far from $\tilde{z}_R^c$), whereas in the unproductive environment the selection gradient on its birth rate would be weak (because the species is near $\tilde{z}_R^c$). This simple example also suggests that many of these predictions may be quite counterintuitive if one were only considering evolutionary features in isolation.

In addition, a critical feature for determining what is favored by natural selection is the differences in strengths of selection gradients experienced by different fitness components (McPeek 1996a). Comparable sets of predictions can be made for the same species in different environmental settings or when comparing different sets of trophic interactors based on the relationships for other model parameters considered in figures 3.8–3.12. A full explanation for patterns of natural selection will require not only quantifying the shapes of fitness surfaces, but also the magnitudes of the associated fitness components and selection gradients on those fitness components, and the abundances and phenotypes of the species that influence those fitness components.

These analyses also highlight that adaptive evolution does not act to perpetuate a species. Species may be incapable of evolving the phenotypes that would be necessary to prevent their extinction. Moreover, adaptive evolution can in some cases favor species to actively move to trait values that will ensure their extinction

(Webb 2003, Parvinen 2005). Adaptive evolution does not act "for the good of the species" overall, and cannot act to make species better at all things. The richness of the study of evolution is embedded in understanding the conflicting ecological and evolutionary demands that any species faces in adapting to the community in which it lives.

UNIFYING FRAMEWORK

The theory pioneered by Lande (1982), Iwasa et al. (1991), and Abrams et al. (1993) for understanding the joint dynamics of species' abundances and traits in a community context (e.g., equations (3.9) and (3.10)) provides a unifying framework for understanding the joint ecological and evolutionary dynamics of a community. The underlying currency is the fitnesses of individuals and how these depend on the abiotic environment in which those individuals find themselves, and the abundances and traits of all the species in the community. The average of these individual fitnesses for each population is the explicit currency that defines the ecological and evolutionary trajectories of all the populations.

In a population dynamics context, we speak of average fitness as the overall per capita demographic rate of the population: dN/Ndt. The average fitness of the population determines whether the abundance will increase, decrease, or not change in the next instant of time.

In an evolutionary context, we speak of average fitness as the fundamental metric of natural selection: $\ln(\bar{W}_N)$. How this will change with a change in the distribution of phenotypes of the population determines whether natural selection can potentially shift that phenotypic distribution (Lande 1982).

Because the symbology of population dynamics and natural selection are different, we typically do not realize that the fundamental basis of both is the same thing; that is, dN/Ndt and $\ln(\bar{W}_N)$ are the same quantity (equation (3.4)), and changes in the abundance of a population and its average trait value are governed by the same basic metric (Charlesworth 1994; Lande 2007, 2008)!

We can see the relationship better by specifying the overall average fitness landscape for a species embedded in a community. The average fitness of a population (i.e., $dN/Ndt = \ln(\bar{W}_N)$) maps onto a system of axes describing the abiotic factors (one subset of axes) for that site, and the abundances (a second subset) and mean traits (a third subset) of this species and all the other species in the community. In this work, I have not explicitly modeled abiotic factors, but rather subsumed their effects into the parameters of the models. In many cases, one would want to also model the dynamics of abiotic factors explicitly, particularly when they have dynamics themselves (e.g., species utilizing resources that can be

depleted, such as water, nitrogen, phosphorus, silica, light). Regardless of whether they can be altered by the actions of the biotic community, the average fitness of a population may change along an abiotic factor axis. As this chapter makes clear for each species in the community, the traits and abundances of all species are also important axes in this system.

To make this discussion concrete and to illustrate visually how ecology and evolution fit together, first consider an extremely simple community composed of a single resource species by itself at a site. Assuming the same relationships for this resource as for all other resources discussed in this chapter, its average fitness is given by

$$\frac{dR}{Rdt} = \ln(\bar{W}_R) = c_0\,(1-\gamma(z_R - \tilde{z}_R^c)^2) - dR, \tag{3.22}$$

with a single bidirectional-independent trait that influences the value of its maximum birth rate, and a linear density-dependent decrease in fitness with increasing abundance (i.e., logistic population growth). Because I am limited to three dimensions, figure 3.13. does not illustrate the abiotic axes that also influence this species' average fitness; because they are not considered explicitly, the fitness surface would change shape as the values of the abiotic factors change. In addition, I am limited to considering only one trait; a full representation would require as many trait axes for this species as it has ecologically important traits. More than one abundance axis would also be needed if this species possessed a complex life cycle with multiple stages. In this illustration, the intrinsic birth optimum is at $\tilde{z}_R^c = 10$. At any point in time, the population of this species is a point in the mean trait-abundance plane, and height of the topography above this point is the average fitness of the individuals in the population. The ecological and evolutionary dynamics of the population move this point as we have described until it eventually reaches the stable equilibrium point of $[R^*, z_R^*] = [50, 10]$.

I show two slicing planes through this three-dimensional fitness topography to illustrate the ecological and evolutionary features driving the dynamics of the population. The first slicing plane runs parallel to the mean trait axis and crosses the abundance axis at $R = 50$; the upper left panel shows the intersection of the fitness surface with this slicing plane (fig. 3.13). This is the relationship between fitness and the mean trait at this abundance, and thus describes phenotypic selection gradients acting on the population for different mean trait values when the abundance of the population is 50. The dynamics of the fitness topography that we explored in this chapter and that we will continue to explore in chapter 5 are simply determined by sliding this slicing plane along the abundance axis as the species' numbers change. Obviously, in more complex communities, the position of the corresponding slicing plane would be moving simultaneously along multiple

trait and abundance axes for all the species, including the species of interest and the abiotic factor axes.

The other slicing plane runs parallel to the abundance axis and crosses the mean trait axis at 10 (fig. 3.13). The intersection of the fitness surface with this slicing plane demarcates where the population abundance would equilibrate given the mean trait value in the population. The equilibrium population abundance, given the current mean trait value, is given by the abundance having $\ln(\bar{W}_{X_i}) = 0$ in the upper right panel; this is a stable equilibrium in this case. If the population abundance is below this value, the abundance will increase, and if above it, population abundance will decrease. It is easy to see why the population would equilibrate at different abundances if the mean trait value in the population changes.

Without boggling the mind too much, now extrapolate this simple picture to the analogous relationship for a multispecies community. The axis system for a community with more interacting species would simply have more mean trait axes and more abundance axes (and don't forget about the abiotic factor axes as well), but we can conceptualize the dynamics of the system in exactly the same way. In fact, I have been doing this throughout this chapter. The per capita population growth forms of equations (3.17)–(3.20) all represent more elaborate multidimensional forms of the figure depicted in figure 3.13*C*, each with more abundance and trait axes. Each species in the community will have a different fitness topography associated with this same multidimensional axis system of abiotic factors and species' traits and abundances, and each species will respond to its own fitness surface associated with this same axis system. A joint abundance and trait equilibrium for the community occurs at each point in these multidimensional spaces where for every species $\ln(\bar{W}) = 0$, and the fitness topography of each and every species at this point has $\partial \ln(W)/\partial z\big|_{z=\bar{z}} = 0$ for all of its own trait axes. The locations of these equilibrium points will define domains of attraction, and within each domain of attraction the species' abundances and traits would either approach the equilibrium (i.e., stable equilibrium) or enter into a limit cycle or chaos of only abundances or of both traits and abundances.

These are the two orientations on which we focus without realizing that they are two perspectives of the same feature. Ecologists take the population regulation perspective (i.e., dR/Rdt vs. abundance in fig. 3.13*B*) and tend to ignore that species' traits are also critical to population dynamics. Likewise, evolutionary biologists take the natural selection perspective (i.e., $\ln(\bar{W}_R)$ vs. mean trait in fig. 3.13*A*) and tend to ignore that the fitnesses of individuals depend on the abundances of all the species in the community. The changing shapes of isoclines and of fitness topographies that we have explored here and will explore further in chapter 5 are simply the result of moving these slicing planes along the axes not considered in each perspective. The shapes of isoclines change as the traits of

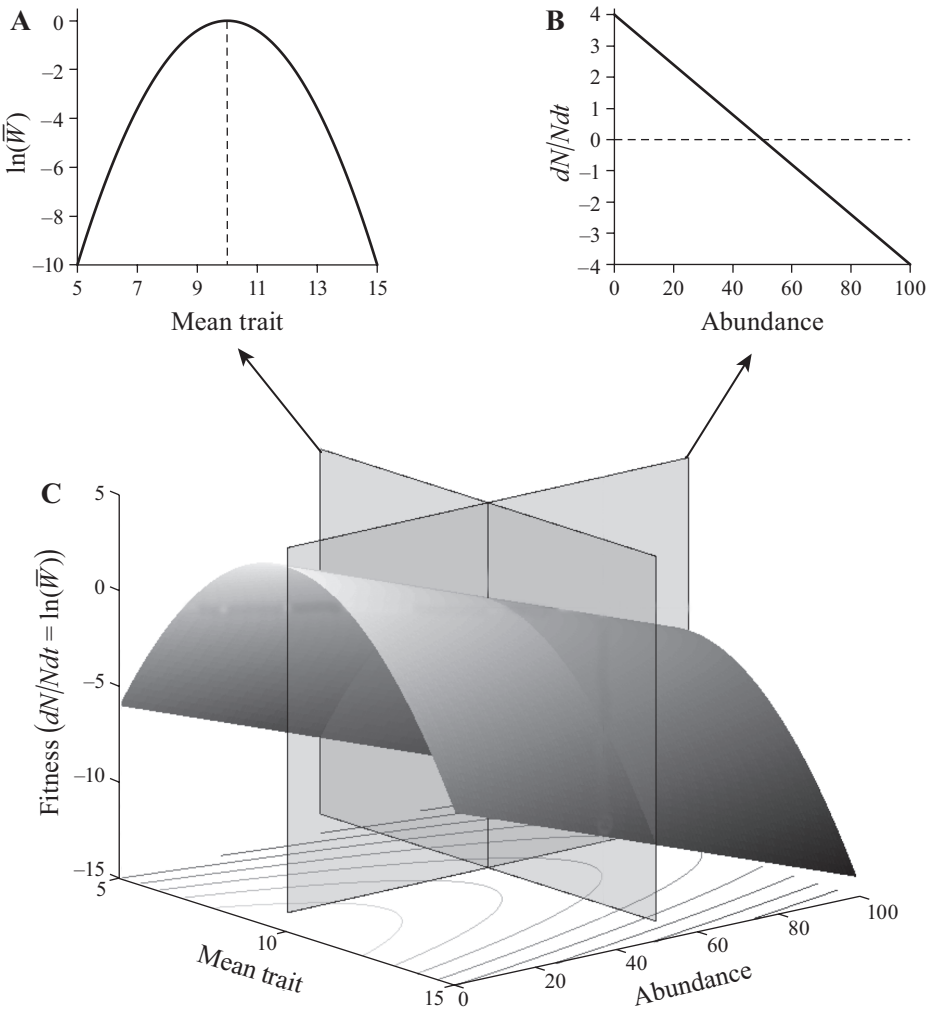

FIGURE 3.13. The fitness surface for a resource species that is the only member of a community, whose average individual fitness is determined by equation (3.22). For this species, the parameters of the model are $c_0 = 4.0$, $d = 0.08$, $\gamma = 0.1$, and $\tilde{z}^c_{X_i} = 10.0$. The *lower* panel shows the fitness surface as a function both the mean trait value in the population and the species' abundance. The *upper left* panel shows the intersection of the fitness surface with the slicing plane at $R = 50$, which is the fitness topography that determines phenotypic selection on this trait at this abundance. The *upper right* panel shows the intersection of the fitness surface with the slicing plane at $z_R = 10.0$, which is the fitness relationship that governs population dynamics at this trait value. (This figure is redrawn from figure 1 of McPeek 2017, with permission.)

the interacting species change (e.g., fig. 3.7), and the shapes of fitness landscapes change as the abundances of all interacting species and the traits of other species change (e.g., fig. 3.3). This conceptual framework plainly reveals that both perspectives are simultaneously essential to understanding either the population dynamics of interacting species or the natural selection of any one species in the community.